

$B - L$ model with $D_4 \times Z_4 \times Z_2$ symmetry for fermion mass hierarchies and mixings

V. V. Vien*

Department of Physics, Tay Nguyen University, Daklak, Vietnam.

(Dated: May 2, 2024)

We construct a gauge $B - L$ model with $D_4 \times Z_4 \times Z_2$ symmetry that can explain the quark and lepton mass hierarchies and their mixings with the realistic CP phases via the type-I seesaw mechanism. Six quark masses, three quark mixing angles and CP phase in the quark sector can get the central values and Yukawa couplings in the quark sector are diluted a range of three orders of magnitude difference by the perturbation theory at the first order. For neutrino sector, the smallness of neutrino mass is achieved by the Type-I seesaw mechanism. Both inverted and normal neutrino mass hierarchies are in consistent with the experimental data. The prediction for the sum of neutrino masses for normal and inverted hierarchies, the effective neutrino masses and the Dirac CP phase are well consistent with all the recent limits.

PACS numbers: 11.30.Hv; 12.15.Ff; 12.60.Cn; 12.60.Fr; 14.60.Pq; 14.60.St

I. INTRODUCTION

The mass hierarchy problem is one of the most exciting issues in particle physics that require the extension of the Standard Model (SM). Some of the experimental data related to flavour problem including the origin of the quark mass hierarchy [1] $m_u \ll m_c \ll m_t$ and $m_d \ll m_s \ll m_b$, the hierarchy of charged lepton mass $m_e \ll m_\mu \ll m_\tau$ and the origin of the tiny of three quark mixing angles as well as the neutrino mass spectrum and mixings.

Because of mentioned issues, various SM extensions have been implemented such as symmetry extensions with scalars and/or fermion fields. The $B - L$ model [2–8] is appreciated because the simplest way is to add three right-handed neutrinos for generating neutrino masses. Although this model solves many interesting problems such as dark matter [3], the muon anomalous magnetic moment [4, 8], leptogenesis [5, 6] and gravitational wave radiation [7], it cannot provide a satisfactory explanation for fermion masses and mixing observables. Non-Abelian discrete symmetries have seem to be the most powerful tool for reproducing the observed mass and mixing patterns of leptona

* vvien@ttn.edu.vn

and quarks (see, for example, Ref. [9]). D_4 symmetry received much attention because it can provide a predictive depiction of the mentioned patterns [10–23], however, those previous works are essentially different from our current study for the following basic points:

- (1) Ref. [16] based on symmetries¹ $G_{BL} \times D_4 \times Z_4$ in which, for the quark sector, up to four $SU(2)_L$ doublets and three singlets are introduced, and the obtained quark mixing matrix, whose "13", "23", "31" and "32" entries are zero, is not natural because in fact all the elements of the quark mixing matrix are non-zero [1].
- (2) Ref. [17] based on symmetries² $G_{SM} \times D_4 \times Z_2$ in which the realistic quark mixing pattern has not been considered and the quark mass hierarchy is not satisfied.
- (3) Ref. [18] based on symmetries $G_{331} \times U(1)_\mathcal{L} \times D_4$ in which five $SU(3)_L$ triplets are used, and the 1 – 2 mixing of the ordinary quarks is obtained if the D_4 symmetry is violated with $1'$ symmetry instead of $\underline{1}$ as usual.
- (4) Ref. [19] based on symmetries $G_{331} \times U(1)_\mathcal{L} \times D_4$ in which the realistic quark mixing matrix is achieved/satisfied, however, the quark mass hierarchy is not satisfied.
- (5) In Ref. [20], the obtained quark mixing matrix, whose "13", "23", "31" and "32" entries are zero, is not natural because in fact all the elements of the quark mixing matrix are non-zero [1], and the quark mass hierarchy is not satisfied.
- (6) In Ref. [21], the obtained quark mixing matrix, whose "13", "23", "31" and "32" entries are zero, is not natural because in fact all the elements of the quark mixing matrix are non-zero [1], and the quark mass hierarchy is not satisfied.
- (7) Ref. [22] based on symmetries $G_{331} \times D_4 \times Z_4 \times Z_3^{(1)} \times Z_3^{(2)} \times Z_{16}$ in which two $SU(3)_L$ triplets and six $SU(3)_L$ singlets are used.
- (8) In Ref. [23], the quark mass hierarchy is a bit unnatural since the Yukawa couplings spread over the region from $\mathcal{O}(10^{-3})$ to $\mathcal{O}(1)$ (three orders of magnitude difference).

Hence, it would be desirable to propose another D_4 flavor model which can overcome the mentioned limitations of previous studies, especially the quark mass hierarchy, the tiny of quark mixing angles, the neutrino mass spectrum and mixing pattern.

¹ $G_{BL} = SU(3)_C \times SU(2)_L \times U(1)_Y \times U(1)_{B-L}$ is the gauge symmetry of $B - L$ model.

² $G_{SM} = SU(3)_C \times SU(2)_L \times U(1)_Y$ is the SM gauge symmetry.

In this study, we propose another D_4 model, which differs from those of Refs. [13, 16], by additionally introducing one doublet (H') put in $\underline{1}'$ under D_4 [13] and using one singlet instead of one doublet in the quark sector [16]. The properties under D_4 of the right handed charged lepton (l_{1R}) and of the right handed neutrino (ν_{1R}), and the properties under Z_4 of right-hand leptons $l_{1R}, l_{\alpha R}, \nu_{1R}, \nu_{\alpha R}$ and singlet scalars χ, φ, ϕ in our present work are completely different from those of Ref. [13, 16]. As a consequence, the charged-leptons, neutrinos and quarks mass hierarchies can be naturally achieved.

The rest of this work is layout as follows. We present the model description in section II. Sections III and IV are devoted to the quark and lepton masses and mixings, respectively. Section V is for the numerical analysis. We make some conclusions in Sec. VI.

II. THE MODEL

The total symmetry of the model is $\Gamma = SU(2)_L \times U(1)_Y \times U(1)_{B-L} \times D_4 \times Z_4 \times Z_2$ where lepton, quark and scalar fields, under D_4 and Z_4 , are essentially different from those of Refs. [13, 16]. Namely, in this study, the first families of the left handed quark, right handed up-and down quarks are assigned in $\mathbf{1}_{+-}$; the two other families of quarks are assigned in $\mathbf{2}$. To explain the hierarchies of quark masses, one $SU(2)_L$ doublet H' with $B-L=0$ put in $\mathbf{1}_{-+}$ under D_4 together with three flavons ρ, φ and ϕ with $B-L=0$ respectively put in $\mathbf{2}$ and $\mathbf{1}_{+-}$ under D_4 are additional introduced, i.e., the considered model contains two $SU(2)_L$ doublets³. The particle and scalar contents of the model is shown in Table I.

Table I. Particle and scalar contents of the model ($\alpha = 2, 3$).

Fields	Q_{1L}	$Q_{\alpha L}$	u_{1R}	$u_{\alpha R}$	d_{1R}	$d_{\alpha R}$	ψ_{1L}	$\psi_{\alpha L}$	l_{1R}	$l_{\alpha R}$	ν_{1R}	$\nu_{\alpha R}$	H	H'	ρ	ϕ	φ	χ
$U(1)_{B-L}$	$\frac{1}{3}$	$\frac{1}{3}$	$\frac{1}{3}$	$\frac{1}{3}$	$\frac{1}{3}$	$\frac{1}{3}$	-1	-1	-1	-1	-1	-1	0	0	0	0	0	2
D_4	$\mathbf{1}_{+-}$	$\mathbf{2}$	$\mathbf{1}_{+-}$	$\mathbf{2}$	$\mathbf{1}_{+-}$	$\mathbf{2}$	$\mathbf{1}_{-+}$	$\mathbf{2}$	$\mathbf{1}_{-+}$	$\mathbf{2}$	$\mathbf{1}_{-+}$	$\mathbf{2}$	$\mathbf{1}_{+-}$	$\mathbf{1}_{-+}$	$\mathbf{2}$	$\mathbf{1}_{+-}$	$\mathbf{1}_{--}$	$\mathbf{1}_{+-}$
Z_4	1	i	-1	$-i$	-1	$-i$	1	i	-1	$-i$	i	i	-1	-1	$-i$	1	-1	-1
Z_2	-	+	-	+	-	+	+	+	+	+	-	-	+	+	-	+	-	+

With the given particle content, $\bar{Q}_{1L}u_{1R}$ transforms as $(\mathbf{2}, \frac{1}{2}, 0, \mathbf{1}_{++}, -1)$ can couple to $(\tilde{H}\phi)_{\mathbf{1}_{++}}$; $\bar{Q}_{\alpha L}u_{\alpha R} \sim (\mathbf{2}, \frac{1}{2}, 0, \mathbf{1}_{+-} + \mathbf{1}_{-+} + \mathbf{1}_{++} + \mathbf{1}_{--}, 1)$ can, respectively, couple to $\tilde{H}, \tilde{H}', (\tilde{H}\phi)_{\mathbf{1}_{++}}$ and $(\tilde{H}'\phi)_{\mathbf{1}_{--}}$; $\bar{Q}_{1L}u_{\alpha R} \sim (\mathbf{2}, \frac{1}{2}, 0, \mathbf{2}, i)$ can couple to $(\tilde{H}\rho)_{\mathbf{2}}$ and $(\tilde{H}'\rho)_{\mathbf{2}}$; and $\bar{Q}_{\alpha L}u_{1R} \sim (\mathbf{2}, \frac{1}{2}, 0, \mathbf{2}, -i)$

³ see, for instance [24, 25], for a review of the two-Higgs-doublet model (2HDM).

can couple to $(\widetilde{H}\rho^*)_{\mathbf{2}}$ and $(\widetilde{H}'\rho^*)_{\mathbf{2}}$ to form invariant terms that generate up-quark mass matrix. The situation is similar to the down quark sector. The Yukawa terms in the quark and lepton sectors are:

$$\begin{aligned}
-\mathcal{L}_Y^q &= \frac{x_1^u}{\Lambda}(\overline{Q}_{1L}u_{1R})_{\mathbf{1}_{++}}(\widetilde{H}\phi)_{\mathbf{1}_{++}} + x_2^u(\overline{Q}_{\alpha L}u_{\alpha R})_{\mathbf{1}_{+-}}\widetilde{H} + x_3^u(\overline{Q}_{\alpha L}u_{\alpha R})_{\mathbf{1}_{-+}}\widetilde{H}' \\
&+ \frac{y_1^u}{\Lambda}(\overline{Q}_{\alpha L}u_{\alpha R})_{\mathbf{1}_{++}}(\widetilde{H}\phi)_{\mathbf{1}_{++}} + \frac{y_2^u}{\Lambda}(\overline{Q}_{\alpha L}u_{\alpha R})_{\mathbf{1}_{--}}(\widetilde{H}'\phi)_{\mathbf{1}_{--}} + \frac{z_1^u}{\Lambda}(\overline{Q}_{1L}u_{\alpha R})_{\mathbf{2}}(\widetilde{H}\rho)_{\mathbf{2}} \\
&+ \frac{z_2^u}{\Lambda}(\overline{Q}_{\alpha L}u_{1R})_{\mathbf{2}}(\widetilde{H}\rho^*)_{\mathbf{2}} + \frac{z_3^u}{\Lambda}(\overline{Q}_{1L}u_{\alpha R})_{\mathbf{2}}(\widetilde{H}'\rho)_{\mathbf{2}} + \frac{z_4^u}{\Lambda}(\overline{Q}_{\alpha L}u_{1R})_{\mathbf{2}}(\widetilde{H}'\rho^*)_{\mathbf{2}} \\
&+ \frac{x_1^d}{\Lambda}(\overline{Q}_{1L}d_{1R})_{\mathbf{1}_{++}}(H\phi)_{\mathbf{1}_{++}} + x_2^d(\overline{Q}_{\alpha L}d_{\alpha R})_{\mathbf{1}_{+-}}H + x_3^d(\overline{Q}_{\alpha L}d_{\alpha R})_{\mathbf{1}_{-+}}H' \\
&+ \frac{y_1^d}{\Lambda}(\overline{Q}_{\alpha L}d_{\alpha R})_{\mathbf{1}_{++}}(H\phi)_{\mathbf{1}_{++}} + \frac{y_2^d}{\Lambda}(\overline{Q}_{\alpha L}d_{\alpha R})_{\mathbf{1}_{--}}(H'\phi)_{\mathbf{1}_{--}} + \frac{z_1^d}{\Lambda}(\overline{Q}_{1L}d_{\alpha R})_{\mathbf{2}}(H\rho)_{\mathbf{2}} \\
&+ \frac{z_2^d}{\Lambda}(\overline{Q}_{\alpha L}d_{1R})_{\mathbf{2}}(H\rho^*)_{\mathbf{2}} + \frac{z_3^d}{\Lambda}(\overline{Q}_{1L}d_{\alpha R})_{\mathbf{2}}(H'\rho)_{\mathbf{2}} + \frac{z_4^d}{\Lambda}(\overline{Q}_{\alpha L}d_{1R})_{\mathbf{2}}(H'\rho^*)_{\mathbf{2}} + \text{H.c.}, \quad (1) \\
-\mathcal{L}_{lep}^Y &= \frac{h_1}{\Lambda}(\overline{\psi}_{1L}l_{1R})_{\mathbf{1}_{++}}(H\phi)_{\mathbf{1}_{++}} + h_2(\overline{\psi}_{\alpha L}l_{\alpha R})_{\mathbf{1}_{+-}}H + h_3(\overline{\psi}_{\alpha L}l_{\alpha R})_{\mathbf{1}_{-+}}H' \\
&+ \frac{h_4}{\Lambda}(\overline{\psi}_{\alpha L}l_{\alpha R})_{\mathbf{1}_{++}}(H\phi)_{\mathbf{1}_{++}} + \frac{h_5}{\Lambda}(\overline{\psi}_{\alpha L}l_{\alpha R})_{\mathbf{1}_{--}}(H'\phi)_{\mathbf{1}_{--}} \\
&+ \frac{x_1}{\Lambda}(\overline{\psi}_{1L}\nu_{\alpha R})_{\mathbf{2}}(\widetilde{H}\rho^*)_{\mathbf{2}} + \frac{x_2}{\Lambda}(\overline{\psi}_{1L}\nu_{\alpha R})_{\mathbf{2}}(\widetilde{H}'\rho^*)_{\mathbf{2}} \\
&+ \frac{x_3}{\Lambda}(\overline{\psi}_{\alpha L}\nu_{\alpha R})_{\mathbf{1}_{-+}}(\widetilde{H}\varphi)_{\mathbf{1}_{-+}} + \frac{x_4}{\Lambda}(\overline{\psi}_{\alpha L}\nu_{\alpha R})_{\mathbf{1}_{+-}}(\widetilde{H}'\varphi)_{\mathbf{1}_{+-}} \\
&+ \frac{y_1}{2\Lambda}(\overline{\nu}_{1R}^c\nu_{1R})_{\mathbf{1}_{++}}(\phi\chi)_{\mathbf{1}_{++}} + y_2(\overline{\nu}_{\alpha R}^c\nu_{\alpha R})_{\mathbf{1}_{+-}}\chi + \frac{y_3}{2\Lambda}(\overline{\nu}_{\alpha R}^c\nu_{\alpha R})_{\mathbf{1}_{++}}(\phi\chi)_{\mathbf{1}_{++}} + \text{H.c.}, \quad (2)
\end{aligned}$$

where $x_{1,2,3}^{u,d}$, $y_{1,2}^{u,d}$ and $z_{1,2,3,4}^{u,d}$ are the Yukawa-like couplings in the quark sector, $h_{1,2,3,4,5}$; $x_{1,2,3,4}$ and $y_{1,2,3}$ are the Yukawa-like couplings in the lepton sector and Λ is the cut-off scale of the theory.

It is worthy to note that additional discrete symmetries D_4 , Z_4 and Z_2 play crucial roles in forbidding undesired terms to get the expected quark and lepton mass matrices which are listed in Table IV. For instance, in the absence of Z_2 , there will be additional invariant terms $(\overline{\psi}_{1L}l_{\alpha R})_{\mathbf{2}}(H\rho)_{\mathbf{2}}$, $(\overline{\psi}_{1L}l_{\alpha R})_{\mathbf{2}}(H'\rho)_{\mathbf{2}}$, $(\overline{\psi}_{\alpha L}l_{1R})_{\mathbf{2}}(H\rho)_{\mathbf{2}}$ and $(\overline{\psi}_{\alpha L}l_{1R})_{\mathbf{2}}(H'\rho)_{\mathbf{2}}$ which contribute to the entries "12", "13", "21" and "31" of the charged lepton matrix. As a result, we cannot obtain the mass of charged leptons as expected since the charged lepton matrix cannot be diagonalized.

The vacuum expectation value (VEV) of the scalar fields get the form:

$$\begin{aligned}
\langle H \rangle &= (0 \quad v)^T, \quad \langle H' \rangle = (0 \quad v')^T, \quad \langle \varphi \rangle = v_\varphi, \quad \langle \phi \rangle = v_\phi, \\
\langle \rho \rangle &= (\langle \rho_1 \rangle, \langle \rho_1 \rangle) \equiv (v_\rho, v_\rho), \quad \langle \chi \rangle = v_\chi. \quad (3)
\end{aligned}$$

In fact, the electroweak symmetry breaking scale is of order about one hundred GeV, $v^2 + v'^2 = (174 \text{ GeV})^2$. Furthermore, in the 2HDM, the limits of the parameter $t_\beta = \frac{v'}{v}$ are given by [26] $t_\beta = \frac{v'}{v} \in [1.0.10.0]$ or [27] $t_\beta = \frac{v'}{v} \in [1.0.3.0]$. For the purpose of determining the scale of Yukawa

couplings, we consider the case of $t_\beta = 1.424$, i.e.,

$$v = 100 \text{ GeV}, \quad v' = 142.40 \text{ GeV}. \quad (4)$$

In addition, in order to satisfy the quark mass hierarchy, the VEV of singlets and the cut-off scale are assumed to be as follows

$$v_\rho = 5 \times 10^{11} \text{ GeV}, \quad v_\phi = 10^{11} \text{ GeV}, \quad \Lambda \simeq 10^{13} \text{ GeV}. \quad (5)$$

The models with more than one $SU(2)_L$ scalar doublet as in this work, the Flavor Changing Neutral Current (FCNC) processes such as $b \rightarrow s\gamma$ exist in the Higgs sector. However, they are suppressed by non-Abelian discrete symmetries [28, 29]. To make such process below the current experimental limits, some restrictions on the model parameters such as the Yukawa couplings and large masses for non SM scalars need to be imposed. The considered model contains many free parameters which allows us freedom to assume that the remaining scalars are sufficiently heavy to fulfil the current experimental limits. Furthermore, the first two lines of Eq. (2) imply that the off-diagonal Yukawa couplings in the charged-lepton sector are proportional to $\frac{v_\phi}{\Lambda} \sim 10^{-2}$. Therefore, the lepton flavor violation (LFV) processes, such as $l_j \rightarrow l_i\gamma$, are suppressed by the tiny factor $\frac{v_\phi}{\Lambda} \frac{1}{m_H}$ associated with the mentioned small Yukawa couplings and the large mass scale of the heavy scalars m_H [30–33]. A detailed study of FCNC and LFV processes are beyond the scope of this work.

III. QUARK MASS AND MIXING

Using the Clebsch-Gordan coefficients of D_4 symmetry [34], from Eq. (1), when the scalar fields get the VEVs as, Eq. (3), the up-and down-quark mass matrices take the following forms:

$$M_q = M_q^{(0)} + \delta M_q \quad (q = u, d), \quad (6)$$

where

$$M_q^{(0)} = \begin{pmatrix} a_{1q} & 0 & 0 \\ 0 & a_{2q} + a_{3q} & 0 \\ 0 & 0 & a_{2q} - a_{3q} \end{pmatrix}, \quad \delta M_q = \begin{pmatrix} 0 & c_{1q} + c_{3q} & c_{1q} - c_{3q} \\ c_{2q} + c_{4q} & 0 & b_{1q} + b_{2q} \\ c_{2q} - c_{4q} & b_{1q} - b_{2q} & 0 \end{pmatrix}, \quad (7)$$

with

$$\begin{aligned} a_{1q} &= x_1^q v \frac{v_\phi}{\Lambda}, & a_{2q} &= x_2^q v, & a_{3q} &= x_3^q v', & b_{1q} &= y_1^q v \frac{v_\phi}{\Lambda}, & b_{2q} &= y_2^q v' \frac{v_\phi}{\Lambda}, \\ c_{1q} &= z_1^q v \frac{v_\rho}{\Lambda}, & c_{2q} &= z_2^q v \frac{v_\rho}{\Lambda}, & c_{3q} &= z_3^q v' \frac{v_\rho}{\Lambda}, & c_{4q} &= z_4^q v' \frac{v_\rho}{\Lambda} \quad (q = u, d). \end{aligned} \quad (8)$$

Expressions (6)–(8) show that, besides two doublets H and H' , one singlet φ contributes to $M_q^{(0)}$ while δM_q is due to the contribution of two singlets ρ and ϕ . Without the contributions of ρ and ϕ , δM_q will be vanished and the quark mass matrices M_q in Eq. (6) reduce to the diagonal matrices $M_q^{(0)}$, i.e., the corresponding quark mixing matrix $V_{CKM} = \mathbb{I}_{3 \times 3}$ which was ruled out by the recent data. The realistic quark mixing angles are very small [1] which implies that the quark mixing matrix is very close to the identity matrix; thus, the second term δM_q in Eq.(7) can be considered as the perturbed parameter for generating the quark mixing pattern. As a consequence, the realistic quark mixing pattern can be achieved at the first order of perturbation theory. Indeed, at the first order of perturbed theory, the matrices δM_q contribute to the eigenvectors but they have no contribution to the eigenvalues of the quark mass matrices M_q . The quark masses are determined as

$$\begin{aligned} m_u &= a_{1u}, \quad m_c = a_{2u} + a_{3u}, \quad m_t = a_{2u} - a_{3u}, \\ m_d &= a_{1d}, \quad m_s = a_{2d} + a_{3d}, \quad m_b = a_{2d} - a_{3d}, \end{aligned} \quad (9)$$

and the corresponding perturbed quark mixing matrices are:

$$U_L^u = U_R^u = \begin{pmatrix} 1 & \frac{c_{1u}+c_{3u}}{m_c-m_u} & \frac{c_{1u}-c_{3u}}{m_t-m_u} \\ \frac{c_{4u}+c_{2u}}{m_u-m_c} & 1 & \frac{b_{2u}+b_{1u}}{m_t-m_c} \\ \frac{c_{4u}-c_{2u}}{m_t-m_u} & \frac{b_{2u}-b_{1u}}{m_t-m_c} & 1 \end{pmatrix}, \quad U_L^d = U_R^d = \begin{pmatrix} 1 & \frac{c_{1d}+c_{3d}}{m_s-m_d} & \frac{c_{1d}-c_{3d}}{m_b-m_d} \\ \frac{c_{4d}+c_{2d}}{m_d-m_s} & 1 & \frac{b_{2d}+b_{1d}}{m_b-m_s} \\ \frac{c_{4d}-c_{2d}}{m_b-m_d} & \frac{b_{2d}-b_{1d}}{m_b-m_s} & 1 \end{pmatrix}, \quad (10)$$

with $b_{1,2q}$ and $c_{1,2,3,4q}$ ($q = u, d$) are given in Eq. (8). For simplicity, we consider the case of $y_{1q} = y_{2q} = y_q$ ($q = u, d$), $z_{3d} = z_{1d} = z_d$, i.e.,

$$b_{2d} = b_{1d} = b_d, \quad b_{2u} = b_{1u} = b_u, \quad c_{3d} = c_{1d}. \quad (11)$$

The quark mixing matrix, $V_{CKM} = V_L^u V_L^{d\dagger}$, owns the following entries:

$$\begin{aligned} V_{CKM}^{11} &= 1 + \frac{2c_{1d}^*(c_{1u} + c_{3u})}{(m_u - m_c)(m_d - m_s)}, \\ V_{CKM}^{12} &= \frac{2b_d^*(c_{1u} - c_{3u})}{(m_b - m_s)(m_t - m_u)} + \frac{c_{1u} + c_{3u}}{m_c - m_u} + \frac{c_{2d}^* + c_{4d}^*}{m_d - m_s}, \\ V_{CKM}^{13} &= \frac{c_{1u} - c_{3u}}{m_t - m_u} + \frac{c_{4d}^* - c_{2d}^*}{m_b - m_d}, \quad V_{CKM}^{21} = \frac{c_{2u} + c_{4u}}{m_u - m_c} + \frac{2c_{1d}^*}{m_s - m_d}, \\ V_{CKM}^{22} &= 1 + \frac{4b_d^* b_u}{(m_b - m_s)(m_t - m_c)} + \frac{(c_{2u} + c_{4u})(c_{2d}^* + c_{4d}^*)}{(m_u - m_c)(m_d - m_s)}, \\ V_{CKM}^{23} &= \frac{2b_u}{m_t - m_c} + \frac{(c_{2u} + c_{4u})(c_{2d}^* - c_{4d}^*)}{(m_b - m_d)(m_c - m_u)}, \quad V_{CKM}^{31} = \frac{c_{4u} - c_{2u}}{m_t - m_u}, \\ V_{CKM}^{32} &= \frac{2b_d^*}{m_b - m_s} + \frac{(c_{2u} - c_{4u})(c_{2d}^* + c_{4d}^*)}{(m_d - m_s)(m_u - m_t)}, \quad V_{CKM}^{33} = 1 + \frac{(c_{2u} - c_{4u})(c_{2d}^* - c_{4d}^*)}{(m_b - m_d)(m_t - m_u)}. \end{aligned} \quad (12)$$

Comparing the model results on the quark masses and quark mixing matrix in Eqs. (9) and (12) with their corresponding experimental constraints on V_{ij}^{exp} as shown in Tab. II (the second column), we get the explicit expressions of $a_{1u,d}$, $a_{2u,d}$, $a_{3u,d}$, $b_{u,d}$, $c_{1u,d}$, $c_{2u,d}$, c_{3u} and $c_{4u,d}$ as functions of quark masses and quark mixing matrix elements as presented in Eqs. (B1) and (B2) of Appendix B.

Expressions (8), (11), (B1) and (B2) imply that the model parameters $a_{1u,d}$, $a_{2u,d}$, $a_{3u,d}$, $b_{u,d}$, $c_{1u,d}$, $c_{2u,d}$, c_{3u} and $c_{4u,d}$ depend on the observed parameters in the quark sector, including quark masses $m_u, m_c, m_t, m_d, m_s, m_b$ and quark mixing matrix elements V_{ij}^{exp} ($i, j = 1, 2, 3$), that have been determined accurately [1]. At the best-fit points of mentioned parameters⁴ given in Refs.[1], we obtain a prediction for the quark mixing matrix and the model's parameters in the quark sector as shown in Table II and Eq. (13), respectively.

Table II. The best-fit points for quark parameters taken from Ref.[1] and the model prediction.

Observable	Best-fit point [1]	The model prediction	Percent error (%)
m_u [MeV]	2.16	2.16	0
m_c [GeV]	1.27	1.27	0
m_t [GeV]	172.69	172.69	0
m_d [MeV]	4.67	4.67	0
m_s [MeV]	93.4	93.4	0
m_b [GeV]	4.18	4.18	0
V_{CKM}^{11}	0.974352	0.974352	0
V_{CKM}^{12}	0.224998	0.224998	0
V_{CKM}^{13}	$0.0015275 - 0.003359i$	$0.0015275 - 0.003359i$	0
V_{CKM}^{21}	$-0.224865 - 0.000136871i$	$-0.224865 - 0.000136871i$	0
V_{CKM}^{22}	0.973492	0.973492	0
V_{CKM}^{23}	0.0418197	0.0418197	0
V_{CKM}^{31}	$0.00792247 - 0.00327i$	$0.00792247 - 0.00327i$	0
V_{CKM}^{32}	$-0.0410911 - 0.000755113i$	$-0.0410911 - 0.000755113i$	0
V_{CKM}^{33}	0.999118	0.999118	0

⁴ The best-fit points in Table II correspond to the Wolfenstein parameters[1]: $\lambda = 0.2250$, $A = 0.826$, $\bar{\rho} = 0.159$ and $\bar{\eta} = 0.348$ which correspond to the mixing angles $\sin \theta_{12}^q = 0.22500$, $\sin \theta_{13}^q = 0.00369$, $\sin \theta_{23}^q = 0.04182$ and $\delta_{CP}^q = 1.444$.

$$\begin{aligned}
a_{1u} &= 2.160 \times 10^{-3} \text{ GeV}, \quad a_{2u} = 86.980 \text{ GeV}, \quad a_{3u} = -85.710 \text{ GeV}, \\
b_u &= (2.308 + 0.5413i) \text{ GeV}, \quad c_{1u} = 8.414 + 3.028i \text{ GeV}, \\
c_{2u} &= (-0.614 + 0.211i) \text{ GeV}, \quad c_{3u} = (-8.269 - 3.170i) \text{ GeV}, \\
c_{4u} &= (0.754 - 0.353i) \text{ GeV}, \quad a_{1d} = 4.670 \times 10^{-3} \text{ GeV}, \quad a_{2d} = 2.140 \text{ GeV}, \\
a_{3d} &= -2.040 \text{ GeV}, \quad b_d = (-8.658 + 0.262i)10^{-2} \text{ GeV}, \\
c_{1d} &= (-5.080 + 4.973i)10^{-3} \text{ GeV}, \quad c_{2d} = (0.193 - 0.077i) \text{ GeV}, \\
c_{4d} &= (-0.204 + 0.087i) \text{ GeV}.
\end{aligned} \tag{13}$$

The Jarlskog invariant in the quark sector, $J_{CP}^q = \text{Im}[V_{us}V_{cb}V_{cs}^*V_{ub}^*]$, is calculated from Eq. (12) with the model result in Table II (the third column) as $J_{CP}^q = 3.08 \times 10^{-5}$, which coincides with that of Ref. [1].

Next, comparing Eqs. (8) and (13) with the aid of Eqs. (4)-(5), ones obtain:

$$\begin{aligned}
|x_{1u}| &= 2.16 \times 10^{-3}, \quad |x_{2u}| = 0.87, \quad |x_{3u}| = 0.60, \quad |y_{1u}| = 2.37, \\
|y_{2u}| &= 1.67, \quad |z_{1u}| = 1.79, \quad |z_{2u}| = 0.13, \quad |z_{3u}| = 1.24, \quad |z_{4u}| = 0.12, \\
|x_{1d}| &= 4.67 \times 10^{-3}, \quad |x_{2d}| = 2.14 \times 10^{-2}, \quad |x_{3d}| = 1.43 \times 10^{-2}, \\
|y_{1d}| &= 8.66 \times 10^{-2}, \quad |y_{2d}| = 6.08 \times 10^{-2}, \quad |z_{1d}| = 1.42 \times 10^{-3}, \\
|z_{2d}| &= 4.16 \times 10^{-2}, \quad |z_{3d}| = 10^{-2}, \quad |z_{4d}| = 3.11 \times 10^{-2},
\end{aligned} \tag{14}$$

which differ by about three orders of magnitude.

IV. LEPTON MASSES AND MIXINGS

Using the Clebsch-Gordan coefficients of D_4 [34], from Eq. (2), when the scalar fields get the VEVs, Eq. (3), we find charged leptons (M_l) and neutrino (Dirac and right-handed Majorana) mass matrices (M_D, M_R) as follows

$$M_l = \begin{pmatrix} a_1 & 0 & 0 \\ 0 & a_2 + a_3 & a_4 + a_5 \\ 0 & a_4 - a_5 & a_2 - a_3 \end{pmatrix}, \quad M_D = \begin{pmatrix} 0 & -a_D + b_D & a_D + b_D \\ 0 & c_D + d_D & 0 \\ 0 & 0 & -c_D + d_D \end{pmatrix}, \quad M_R = \begin{pmatrix} a_R & 0 & 0 \\ 0 & b_R & c_R \\ 0 & c_R & b_R \end{pmatrix}, \tag{15}$$

where

$$a_1 = \left(\frac{v_\phi}{\Lambda}\right) v h_1, \quad a_2 = h_2 v, \quad a_3 = h_3 v', \quad a_4 = \left(\frac{v_\phi}{\Lambda}\right) v h_4, \quad a_5 = \left(\frac{v_\phi}{\Lambda}\right) v' h_5. \quad (16)$$

$$a_D = \left(\frac{v_\rho}{\Lambda}\right) x_1 v, \quad b_D = \left(\frac{v_\rho}{\Lambda}\right) x_2 v', \quad c_D = \left(\frac{v_\varphi}{\Lambda}\right) x_3 v, \quad d_D = \left(\frac{v_\varphi}{\Lambda}\right) x_4 v',$$

$$a_R = \frac{y_1}{\Lambda} v_\chi v_\phi, \quad b_R = y_2 v_\chi, \quad c_R = \frac{y_3}{\Lambda} v_\chi v_\phi. \quad (17)$$

• *Charged-lepton sector:* For simplicity, we consider the case of $\arg h_3 = (\arg h_2 + \pi)$ and $\arg h_5 = \arg h_4$, i.e, $\arg a_3 = (\arg a_2 + \pi)$ and $\arg a_5 = \arg a_4$. Yukawa couplings h_i ($i = 1 \div 5$) are complex in general, therefore the matrix M_l is complex and its eigenvalues are complex. Let us first define a Hermitian matrix $m_l^2 = M_l M_l^\dagger$, given by

$$m_l^2 = M_l M_l^\dagger = \begin{pmatrix} A_0 & 0 & 0 \\ 0 & B_0 & \mathcal{D}_0 \cdot e^{-i\theta} \\ 0 & \mathcal{D}_0 \cdot e^{i\theta} & C_0 \end{pmatrix}, \quad (18)$$

where⁵

$$A_0 = |a_1|^2, \quad B_0 = (|a_2| - |a_3|)^2 + (|a_4| + |a_5|)^2, \quad C_0 = (|a_2| + |a_3|)^2 + (|a_4| - |a_5|)^2,$$

$$D_0 = 2(|a_2||a_4| + |a_3||a_5|)c_\alpha, \quad G_0 = -2(|a_3||a_4| + |a_2||a_5|)s_\alpha, \quad \mathcal{D}_0 = \sqrt{D_0^2 + G_0^2}, \quad (19)$$

$$\theta = \arccos\left(\frac{D_0}{\mathcal{D}_0}\right), \quad \alpha = \arg a_2 - \arg a_4. \quad (20)$$

The matrix m_l^2 in Eq. (18) is diagonalised by two mixing matrices $V_{l(L,R)}$ with $V_{lL}^+ m_l^2 V_{lR} = \text{diag}(m_e^2, m_\mu^2, m_\tau^2)$, where

$$m_e^2 = A_0, \quad m_{\mu,\tau}^2 = \frac{1}{2} \left(B_0 + C_0 \mp \sqrt{(B_0 - C_0)^2 + 4\mathcal{D}_0^2} \right), \quad (21)$$

$$V_{lL} = V_{lR} = \begin{pmatrix} 1 & 0 & 0 \\ 0 & c_\psi & -s_\psi \cdot e^{-i\theta} \\ 0 & s_\psi \cdot e^{i\theta} & c_\psi \end{pmatrix}, \quad (22)$$

where

$$s_\psi = \frac{1}{\sqrt{2} \sqrt{1 - \frac{B_0 - C_0}{B_0 - C_0 + \sqrt{(B_0 - C_0)^2 + 4\mathcal{D}_0^2}}}}. \quad (23)$$

Equations (19)-(21) and (23) yield the following relations:

$$|a_1| = m_e, \quad |a_2| = \frac{|a_4| D_0 s_\alpha + |a_5| c_\alpha G_0}{(|a_4|^2 - |a_5|^2) s_{2\alpha}}, \quad |a_3| = \frac{|a_4| c_\alpha G_0 + |a_5| D_0 s_\alpha}{(|a_5|^2 - |a_4|^2) s_{2\alpha}},$$

$$|a_4| = \frac{a+b}{2}, \quad |a_5| = \frac{a-b}{2}, \quad (24)$$

⁵ In this work, the following notations are used: $s_\psi = \sin \psi$, $c_\psi = \cos \psi$, $s_\theta = \sin \theta$, $c_\theta = \cos \theta$, $t_\alpha = \tan \alpha$, $t_\theta = \tan \theta$, $s_\delta = \sin \delta_{CP}$, $s_{ij} = \sin \theta_{ij}$, $c_{ij} = \cos \theta_{ij}$ and $t_{ij} = \tan \theta_{ij}$ ($ij = 12, 13, 23$).

where

$$a = \sqrt{\frac{\sqrt{(B_0 C_0 - x_0 + y_0)^2 - 4B_0 C_0 y_0} + B_0 C_0 - x_0 + y_0}{2C_0}},$$

$$b = \sqrt{\frac{\sqrt{(B_0 C_0 - x_0 + y_0)^2 - 4B_0 C_0 y_0} + B_0 C_0 + x_0 - y_0}{2B_0}}, \quad (25)$$

$$x_0 = \frac{(c_\alpha G_0 + D_0 s_\alpha)^2}{s_{2\alpha}^2}, \quad y_0 = \frac{(c_\alpha G_0 - D_0 s_\alpha)^2}{s_{2\alpha}^2}, \quad (26)$$

$$B_0 = (m_\mu^2 - m_\tau^2) s_\psi^2 + m_\tau^2, \quad C_0 = (m_\mu^2 - m_\tau^2) s_\psi^2 + m_\mu^2,$$

$$D_0 = (m_\tau^2 - m_\mu^2) c_\theta s_\psi c_\psi, \quad G_0 = (m_\mu^2 - m_\tau^2) s_\theta s_\psi c_\psi. \quad (27)$$

Expressions (16) and (24)-(27) imply that h_1 depends on m_e, Λ, v_ϕ and v ; h_2 depends on $v, m_\mu, m_\tau, \psi, \theta$ and α ; h_3 depends on $v', m_\mu, m_\tau, \psi, \theta$ and α ; and h_4 and h_5 depend on $v, \Lambda, v_\phi, m_\mu, m_\tau, \psi, \theta$ and α . As will see in Sec. V, with the observed charged leptons $m_{e,\mu,\tau}$ [1] and the cut-off scale, the VEV scales of scalar fields in Eqs (4) and (5), there exist possible ranges of the model parameters such that the Yukawa couplings in the charged lepton sector, h_i ($i = 1 \div 5$), differ by about two orders of magnitude, i.e., the charged lepton mass hierarchy is satisfied.

• *Neutrino sector:* The effective neutrino mass matrix arise from type-I seesaw mechanism $M_\nu = -M_D M_R^{-1} M_D^T$, obtained from Eq. (15), as follows:

$$M_\nu = \begin{pmatrix} A & -B_1 & -B_2 \\ -B_1 & C_1 & C_3 \\ -B_2 & C_3 & C_2 \end{pmatrix}, \quad (28)$$

where

$$A = \frac{2b_D^2}{b_R + c_R} + \frac{2a_D^2}{b_R - c_R}, \quad B_1 = \frac{(c_D + d_D)[a_D(b_R + c_R) - b_D(b_R - c_R)]}{b_R^2 - c_R^2},$$

$$B_2 = \frac{(c_D - d_D)[a_D(b_R + c_R) + b_D(b_R - c_R)]}{b_R^2 - c_R^2}, \quad C_1 = \frac{b_R(c_D + d_D)^2}{b_R^2 - c_R^2},$$

$$C_2 = \frac{b_R(c_D - d_D)^2}{b_R^2 - c_R^2}, \quad C_3 = \frac{c_R(c_D^2 - d_D^2)}{b_R^2 - c_R^2}. \quad (29)$$

The mass matrix M_ν in Eq.(28) owns three eigenvalues and the corresponding mixing matrix as

follows:

$$\lambda_1 = 0, \quad \lambda_2 = \frac{C_2 - 2B_2n_1 + An_1^2 + n_2(2C_3 - 2B_1n_1 + C_1n_2)}{n_1^2 + n_2^2 + 1},$$

$$\lambda_3 = \frac{C_2 - 2B_2t_1 + At_1^2 + t_2(2C_3 - 2B_1t_1 + C_1t_2)}{t_1^2 + t_2^2 + 1}, \quad (30)$$

$$R = \begin{pmatrix} \frac{k_1}{\sqrt{1+k_1^2(1+k_2^2)}} & \frac{n_1}{\sqrt{n_1^2+n_2^2+1}} & \frac{t_1}{\sqrt{t_1^2+t_2^2+1}} \\ \frac{k_1k_2}{\sqrt{1+k_1^2(1+k_2^2)}} & \frac{n_2}{\sqrt{n_1^2+n_2^2+1}} & \frac{t_2}{\sqrt{t_1^2+t_2^2+1}} \\ \frac{1}{\sqrt{1+k_1^2(1+k_2^2)}} & \frac{1}{\sqrt{n_1^2+n_2^2+1}} & \frac{1}{\sqrt{t_1^2+t_2^2+1}} \end{pmatrix}, \quad (31)$$

where new parameters $k_{1,2}, n_{1,2}$ and $t_{1,2}$, own explicit expressions in Appendix C, satisfy the following relations

$$k_1(n_1 + k_2n_2) + 1 = 0, \quad k_1(t_1 + k_2t_2) + 1 = 0, \quad n_1t_1 + n_2t_2 + 1 = 0, \quad (32)$$

$$C_2 - B_2(k_1 + n_1) + C_3(k_1k_2 + n_2) + k_1[An_1 + C_1k_2n_2 - B_1(k_2n_1 + n_2)] = 0, \quad (33)$$

$$C_2 - B_2(k_1 + t_1) + C_3(k_1k_2 + t_2) + k_1[At_1 + C_1k_2t_2 - B_1(k_2t_1 + t_2)] = 0, \quad (34)$$

$$C_2 + C_3n_2 + An_1t_1 - B_1n_2t_1 - B_2(n_1 + t_1) + (C_3 - B_1n_1 + C_1n_2)t_2 = 0, \quad (35)$$

$$C_2 + k_1[2C_3k_2 - 2B_2 + k_1(A - 2B_1k_2 + C_1k_2^2)] = 0. \quad (36)$$

Depending on the sign of Δm_{31}^2 , the neutrino mass spectrum can be normal or inverted hierarchy [1]. In the considered model, $0 = m_1 \equiv \lambda_1 < m_2 \equiv \lambda_2 < m_3 \equiv \lambda_3$ for NH and $0 = m_3 \equiv \lambda_1 < m_1 \equiv \lambda_2 < m_2 \equiv \lambda_3$ for IH. Since the lightest neutrino mass is equal to zero, other neutrino masses and their sum are given by

$$\begin{cases} m_1 = 0, & m_2 = \sqrt{\Delta m_{21}^2}, & m_3 = \sqrt{\Delta m_{31}^2} \text{ for NH,} \\ m_1 = \sqrt{-\Delta m_{31}^2}, & m_2 = \sqrt{\Delta m_{21}^2 - \Delta m_{31}^2}, & m_3 = 0 \text{ for IH.} \end{cases} \quad (37)$$

$$\sum m_\nu = \begin{cases} \sqrt{\Delta m_{21}^2} + \sqrt{\Delta m_{31}^2} \text{ for NH,} \\ \sqrt{\Delta m_{21}^2 - \Delta m_{31}^2} + \sqrt{-\Delta m_{31}^2} \text{ for IH.} \end{cases} \quad (38)$$

The neutrino mass matrix M_ν in Eq. (28) is diagonalized as

$$U_\nu^T M_\nu U_\nu = \begin{cases} \begin{pmatrix} 0 & 0 & 0 \\ 0 & m_2 & 0 \\ 0 & 0 & m_3 \end{pmatrix}, & U_\nu = \begin{pmatrix} \frac{k_1}{\sqrt{1+k_1^2(1+k_2^2)}} & \frac{n_1}{\sqrt{n_1^2+n_2^2+1}} & \frac{t_1}{\sqrt{t_1^2+t_2^2+1}} \\ \frac{k_1k_2}{\sqrt{1+k_1^2(1+k_2^2)}} & \frac{n_2}{\sqrt{n_1^2+n_2^2+1}} & \frac{t_2}{\sqrt{t_1^2+t_2^2+1}} \\ \frac{1}{\sqrt{1+k_1^2(1+k_2^2)}} & \frac{1}{\sqrt{n_1^2+n_2^2+1}} & \frac{1}{\sqrt{t_1^2+t_2^2+1}} \end{pmatrix} \text{ for NH,} \\ \begin{pmatrix} m_1 & 0 & 0 \\ 0 & m_2 & 0 \\ 0 & 0 & 0 \end{pmatrix}, & U_\nu = \begin{pmatrix} \frac{n_1}{\sqrt{n_1^2+n_2^2+1}} & \frac{t_1}{\sqrt{t_1^2+t_2^2+1}} & \frac{k_1}{\sqrt{1+k_1^2(1+k_2^2)}} \\ \frac{n_2}{\sqrt{n_1^2+n_2^2+1}} & \frac{t_2}{\sqrt{t_1^2+t_2^2+1}} & \frac{k_1k_2}{\sqrt{1+k_1^2(1+k_2^2)}} \\ \frac{1}{\sqrt{n_1^2+n_2^2+1}} & \frac{1}{\sqrt{t_1^2+t_2^2+1}} & \frac{1}{\sqrt{1+k_1^2(1+k_2^2)}} \end{pmatrix} \text{ for IH,} \end{cases} \quad (39)$$

where $\lambda_2, \lambda_3, k_{1,2}, n_{1,2}$ and $t_{1,2}$ are given in Appendix C.

Expressions (30) and (32)-(36) yield:

$$\begin{cases} k_1 = \frac{n_1 t_1 + n_2^2 + 1}{t_1 (n_1^2 + n_2^2) + n_1}, & k_2 = \frac{n_2 (t_1 - n_1)}{n_1 t_1 + n_2^2 + 1}, & t_2 = -\frac{n_1 t_1 + 1}{n_2} & \text{for NH,} \\ n_2 = \frac{1 - k_1 n_1}{k_1 k_2}, & t_1 = \frac{k_1 (n_1 - k_1 k_2^2) - 1}{k_1 [k_1 (1 + k_2^2) n_1 - 1]}, & t_2 = \frac{k_2 (k_1 + n_1)}{-1 + k_1 (1 + k_2^2) n_1} & \text{for IH,} \end{cases} \quad (40)$$

$$A = -\frac{C_2 - B_2(k_1 + n_1) + C_1 k_1 k_2 n_2 + C_3(k_1 k_2 + n_2) - B_1 k_1 (k_2 n_1 + n_2)}{k_1 n_1} \quad (\text{NH and IH}), \quad (41)$$

$$B_1 = \frac{C_3 + C_1 k_1 k_2}{k_1} + \frac{(C_2 - B_2 k_1 + C_3 k_1 k_2)(n_1 - t_1)}{(n_1 t_2 - n_2 t_1) k_1} \quad (\text{NH and IH}), \quad (42)$$

$$B_2 = \frac{C_2}{k_1} + C_3 k_2 \quad (\text{NH and IH}), \quad (43)$$

$$C_1 = \frac{C_3(k_1 - n_1) + \frac{(C_2 - B_2 n_1 + C_3 n_2)(k_1 - t_1)}{t_2 - k_2 t_1} + \frac{(C_2 - B_2 k_1 + C_3 k_1 k_2)(n_1 - t_1) n_1}{n_2 t_1 - n_1 t_2}}{k_1 (k_2 n_1 - n_2)} \quad (\text{NH and IH}), \quad (44)$$

$$C_2 = \begin{cases} \frac{\sqrt{\Delta m_{21}^2}}{1 + n_1^2 + n_2^2} + \frac{\sqrt{\Delta m_{31}^2} n_2}{(1 + n_1 t_1)^2 + n_2^2 (1 + t_1^2)} & \text{for NH,} \\ k_1^2 \left(\frac{k_2^2 (\sqrt{-\Delta m_{31}^2} - \sqrt{\Delta m_{21}^2 - \Delta m_{31}^2})}{1 + 2k_1 n_1 + k_1^2 [n_1^2 + k_2^2 (1 + n_1^2)]} + \frac{(1 + k_2^2) \sqrt{\Delta m_{21}^2 - \Delta m_{31}^2}}{1 + k_1^2 (1 + k_2^2)} \right) & \text{for IH,} \end{cases} \quad (45)$$

$$C_3 = \begin{cases} \frac{\sqrt{\Delta m_{21}^2} n_2}{1 + n_1^2 + n_2^2} - \frac{\sqrt{\Delta m_{31}^2} (1 + n_1 t_1) n_2}{(1 + n_1 t_1)^2 + n_2^2 (1 + t_1^2)} & \text{for NH,} \\ k_1 k_2 \left(\frac{(\sqrt{\Delta m_{21}^2 - \Delta m_{31}^2} - \sqrt{-\Delta m_{31}^2}) (k_1 n_1 + 1)}{1 + 2k_1 n_1 + k_1^2 [n_1^2 + k_2^2 (1 + n_1^2)]} - \frac{\sqrt{\Delta m_{21}^2 - \Delta m_{31}^2}}{1 + k_1^2 (1 + k_2^2)} \right) & \text{for IH.} \end{cases} \quad (46)$$

The corresponding leptonic mixing matrix is

$$U = U_L^\dagger U_\nu = \begin{cases} \begin{pmatrix} \frac{k_1}{\sqrt{(k_2^2 + 1)k_1^2 + 1}} & \frac{n_1}{\sqrt{n_1^2 + n_2^2 + 1}} & \frac{t_1}{\sqrt{t_1^2 + t_2^2 + 1}} \\ \frac{c_\psi k_1 k_2 + e^{-i\theta} s_\psi}{\sqrt{(k_2^2 + 1)k_1^2 + 1}} & e^{-i\theta} (c_\psi e^{i\theta} n_2 + s_\psi) & e^{-i\theta} (s_\psi + e^{i\theta} c_\psi t_2) \\ \frac{c_\psi - e^{i\theta} k_1 k_2 s_\psi}{\sqrt{(k_2^2 + 1)k_1^2 + 1}} & \frac{c_\psi - e^{i\theta} n_2 s_\psi}{\sqrt{n_1^2 + n_2^2 + 1}} & \frac{c_\psi - e^{i\theta} s_\psi t_2}{\sqrt{t_1^2 + t_2^2 + 1}} \end{pmatrix} & \text{for NH,} \\ \begin{pmatrix} \frac{n_1}{\sqrt{n_1^2 + n_2^2 + 1}} & \frac{t_1}{\sqrt{t_1^2 + t_2^2 + 1}} & \frac{k_1}{\sqrt{(k_2^2 + 1)k_1^2 + 1}} \\ e^{-i\theta} (c_\psi e^{i\theta} n_2 + s_\psi) & e^{-i\theta} (s_\psi + e^{i\theta} c_\psi t_2) & \frac{c_\psi k_1 k_2 + e^{-i\theta} s_\psi}{\sqrt{(k_2^2 + 1)k_1^2 + 1}} \\ \frac{c_\psi - e^{i\theta} n_2 s_\psi}{\sqrt{n_1^2 + n_2^2 + 1}} & \frac{c_\psi - e^{i\theta} s_\psi t_2}{\sqrt{t_1^2 + t_2^2 + 1}} & \frac{c_\psi - e^{i\theta} k_1 k_2 s_\psi}{\sqrt{(k_2^2 + 1)k_1^2 + 1}} \end{pmatrix} & \text{for IH.} \end{cases} \quad (47)$$

The lepton mixing matrix U_{PMNS} , in the standard parametrization, take the form:

$$U_{\text{PMNS}} = \begin{pmatrix} c_{13} c_{12} & s_{12} c_{13} & s_{13} e^{-i\delta} \\ -c_{23} s_{12} - e^{i\delta} c_{12} s_{13} s_{23} & c_{12} c_{23} - e^{i\delta} s_{12} s_{13} s_{23} & c_{13} s_{23} \\ s_{12} s_{23} - e^{i\delta} c_{12} c_{23} s_{13} & -c_{12} s_{23} - e^{i\delta} c_{23} s_{12} s_{13} & c_{13} c_{23} \end{pmatrix} \begin{pmatrix} 1 & 0 & 0 \\ 0 & e^{i\eta_1} & 0 \\ 0 & 0 & e^{i\eta_2} \end{pmatrix}, \quad (48)$$

where $s_{ij} = \sin \theta_{ij}$ and $c_{ij} = \cos \theta_{ij}$ with θ_{13}, θ_{12} and θ_{23} are the reactor, solar and atmospheric mixing angles, respectively; δ_{CP} is the Dirac CP violation phase and $\eta_{1,2}$ are the two Majorana CP

violating phases. Comparing the entries "12" and "13" of two mixing matrices in (47) and (48) we get:

$$\eta_1 = 0, \eta_2 = \delta \quad (\text{both NH and IH}). \quad (49)$$

The lepton mixing angles, obtained from Eqs. (47) and (48), are:

$$s_{13}^2 = |U_{e3}|^2 = \begin{cases} \frac{t_1^2}{t_1^2 + t_2^2 + 1} & \text{for NH,} \\ \frac{k_1^2}{1 + k_1^2(1 + k_2^2)} & \text{for IH,} \end{cases} \quad (50)$$

$$s_{12}^2 = \frac{|U_{e2}|^2}{1 - |U_{e3}|^2} = \begin{cases} \frac{n_1^2(t_1^2 + t_2^2 + 1)}{(t_2^2 + 1)(n_1^2 + n_2^2 + 1)} & \text{for NH,} \\ \frac{[1 + k_1^2(1 + k_2^2)]t_1^2}{(1 + k_1^2k_2^2)(1 + t_1^2 + t_2^2)} & \text{for IH,} \end{cases} \quad (51)$$

$$s_{23}^2 = \frac{|U_{\mu 3}|^2}{1 - |U_{e3}|^2} = \begin{cases} \frac{c_\psi^2 t_2^2 + s_{2\psi} c_\theta t_2 + s_\psi^2}{t_2^2 + 1} & \text{for NH,} \\ \frac{c_\psi^2 k_1^2 k_2^2 + s_\psi^2 + k_1 k_2 s_{2\psi} c_\theta}{1 + k_1^2 k_2^2} & \text{for IH,} \end{cases} \quad (52)$$

The Jarlskog invariant in the active sector, determined from Eq. (47), takes the form [1, 35]

$$J_{CP}^{(l)} = \frac{n_1 t_1 (t_2 - n_2) s_\psi c_\psi s_\theta}{(n_1^2 + n_2^2 + 1) (1 + t_1^2 + t_2^2)} \quad (\text{NH and IH}). \quad (53)$$

Comparing $J_{CP}^{(l)}$ in Eq. (53) and that of the standard parametrization, $J_{CP}^{(l)} = c_{12} c_{13}^2 c_{23} s_{12} s_{13} s_{23} s_\delta$, we obtain:

$$s_\delta = \frac{n_1 t_1 (t_2 - n_2) s_\psi c_\psi s_\theta}{(n_1^2 + n_2^2 + 1) (1 + t_1^2 + t_2^2) c_{12} c_{13}^2 c_{23} s_{12} s_{13} s_{23}} \quad (\text{NH and IH}). \quad (54)$$

The effective neutrino masses [36], obtained from Eqs. (37), (39) and (47), possess the following forms:

$$\langle m_{ee} \rangle = \left| \sum_{i=1}^3 U_{ei}^2 m_i \right| = \begin{cases} \frac{\sqrt{\Delta m_{21}^2} n_1^2}{1 + n_1^2 + n_2^2} + \frac{\sqrt{\Delta m_{31}^2} t_1^2}{1 + t_1^2 + t_2^2} & \text{for NH,} \\ \frac{\sqrt{-\Delta m_{31}^2} n_1^2}{1 + n_1^2 + n_2^2} + \frac{\sqrt{\Delta m_{21}^2 - \Delta m_{31}^2} t_1^2}{1 + t_1^2 + t_2^2} & \text{for IH,} \end{cases} \quad (55)$$

$$m_\beta = \sqrt{\sum_{i=1}^3 |U_{ei}|^2 m_i^2} = \begin{cases} \sqrt{\frac{\Delta m_{21}^2 n_1^2}{1 + n_1^2 + n_2^2} + \frac{\Delta m_{31}^2 t_1^2}{1 + t_1^2 + t_2^2}} & \text{for NH,} \\ \sqrt{\frac{(\Delta m_{21}^2 - \Delta m_{31}^2) t_1^2}{1 + t_1^2 + t_2^2} - \frac{\Delta m_{31}^2 n_1^2}{1 + n_1^2 + n_2^2}} & \text{for IH,} \end{cases} \quad (56)$$

From Eqs. (50)-(52), we can express $n_{1,2}, t_1$ and s_δ in terms of two constrained parameters c_θ, s_ψ and five observable parameters $\Delta m_{21}^2, \Delta m_{31}^2, s_{12}^2, s_{23}^2, s_{13}^2$ and as follows:

- For NH:

$$n_1 = \frac{s_{12}^2 c_{13}^4 t_1^2}{\sqrt{(c_{13}^2 t_1^2 - s_{13}^2) s_{12}^2 c_{12}^2 c_{13}^4 t_1^2 - s_{12}^2 s_{13}^2 c_{13}^2 t_1}}, \quad n_2 = \frac{(1 + n_1 t_1) s_{13}}{\sqrt{c_{13}^2 t_1^2 - s_{13}^2}}, \quad (57)$$

$$t_1 = t_{13} \sqrt{\frac{s_\psi^2 (s_{23}^2 - c_\psi^2) + c_\psi^2 (c_{23}^2 + c_{2\theta} s_\psi^2) + 2\sqrt{c_\theta^2 c_\psi^2 s_\psi^2 (s_{23}^2 c_{23}^2 - s_\psi^2 c_\psi^2 s_\theta^2)}}{(c_\psi^2 - s_{23}^2)^2}}. \quad (58)$$

- For IH:

$$k_1 = -t_{13} \sqrt{\frac{s_\psi^2(s_{23}^2 - c_\psi^2) + c_\psi^2(c_{23}^2 + c_{2\theta}s_\psi^2) - 2\sqrt{c_\theta^2 c_\psi^2 s_\psi^2 (s_{23}^2 c_{23}^2 - s_\psi^2 c_\psi^2 s_\theta^2)}}{(c_\psi^2 - s_{23}^2)^2}}, \quad (59)$$

$$k_2 = \frac{\sqrt{k_1^2 c_{13}^2 - s_{13}^2}}{k_1 s_{13}}, \quad n_1 = \frac{s_{12} c_{12} c_{13}^2 \sqrt{k_1^2 (k_1^2 c_{13}^2 - s_{13}^2) - k_1 c_{12}^2 s_{13}^2 c_{13}^2}}{s_{13}^4 + s_{12}^2 c_{13}^2 (s_{13}^2 - k_1^2)}. \quad (60)$$

Expressions (40)-(46) and (54)-(60) show that the model parameters $s_\delta, k_{1,2}, n_{1,2}$ and $t_{1,2}$ depend on two constrained parameters c_θ, s_ψ and three observable parameters $s_{12}^2, s_{23}^2, s_{13}^2$ while $A, B_{1,2}, C_{1,2,3}, \langle m_{ee} \rangle$ and m_β depend on two constrained parameters c_θ, s_ψ and five observable parameters $\Delta m_{21}^2, \Delta m_{31}^2, s_{12}^2, s_{23}^2, s_{13}^2$.

V. NUMERICAL ANALYSIS

- *For the charged lepton sector*, using the values of Λ , the observed values of the charged lepton masses [1], $m_e = 0.51099$ MeV, $m_\mu = 105.65837$ MeV, $m_\tau = 1776.86$ MeV and the VEV of scalar fields in Eqs. (4) and (5), with the help of Eqs. (16) and (24)-(27), we get $|h_1| \simeq 10^{-2}$, and $h_{2,3,4,5}$ are still depend on three parameters α, θ and ψ . In the case of $s_\alpha = -0.95$ ($\alpha = 288.2^\circ$), the Yukawa-like couplings $h_{2,3,4,5}$ depend on two parameters θ and ψ which are plotted in Figs. 1 and 2.

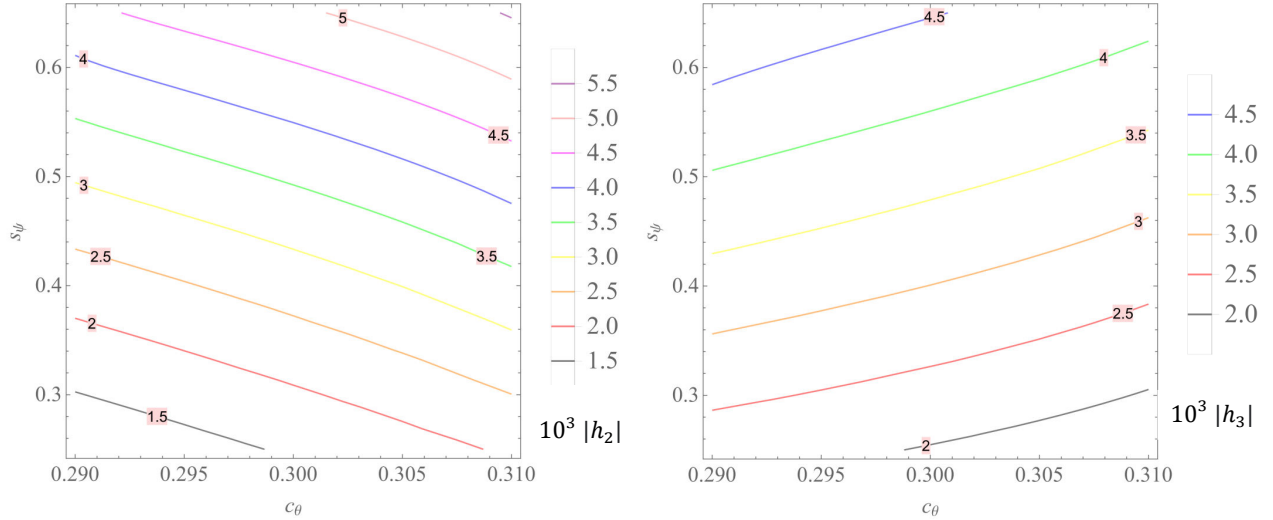


Figure 1. $10^3|h_2|$ (left panel) and $10^3|h_3|$ (right panel) versus c_θ and s_ψ with $c_\theta \in (0.29, 0.31)$ and $s_\psi \in (0.25, 0.65)$.

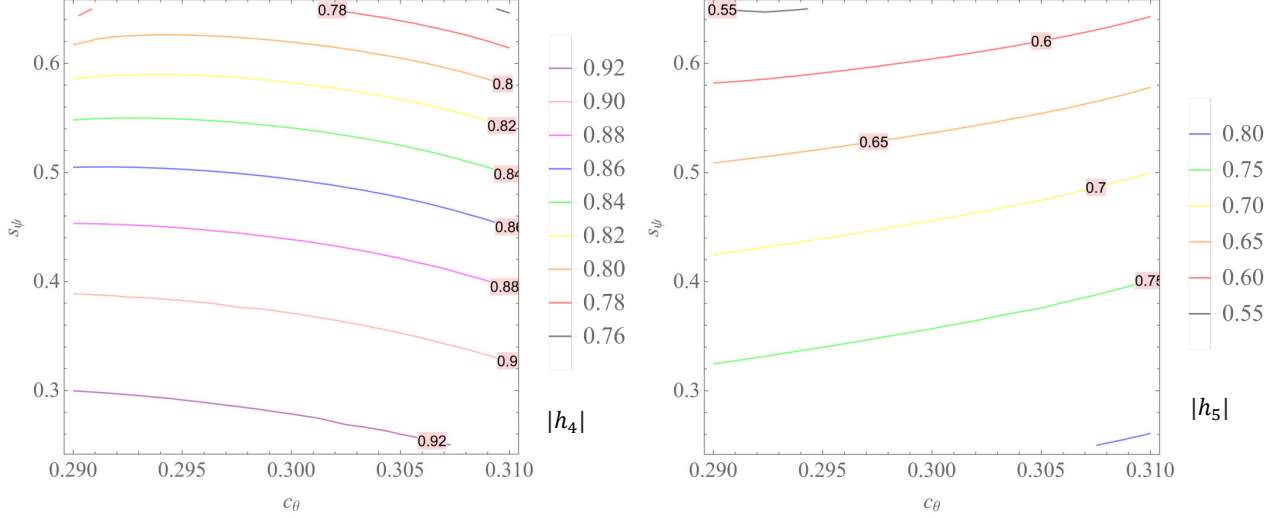


Figure 2. $|h_4|$ (left panel) and $|h_5|$ (right panel) versus c_θ and s_ψ with $c_\theta \in (0.29, 0.31)$ and $s_\psi \in (0.25, 0.65)$.

Figures 1 and 2 imply

$$|h_2| \simeq |h_3| \sim 10^{-2}, \quad |h_4| \simeq |h_5| \sim 10^{-1}, \quad (61)$$

which implies that the Yukawa couplings in the charged lepton sector differ from each other by one order of magnitude for a natural explanation to the charged lepton mass hierarchy.

• *For neutrino sector.* Equation (37) shows that neutrino masses ($m_{2,3}$ for NH and $m_{1,2}$ for IH) depend on two experimental parameters Δm_{31}^2 and Δm_{21}^2 which have been measured with high accuracy. In the case of Δm_{21}^2 and Δm_{31}^2 lie in 3σ range [37], i.e., $\Delta m_{21}^2 \in (69.40, 81.40) \text{ meV}^2$ and $\Delta m_{31}^2 \in (2.47, 3.63) 10^3 \text{ meV}^2$, we get the allowed regions for $m_{1,2,3}$, $m_1 = 0$, $m_2 \in (8.33, 9.02) \text{ meV}$, $m_3 = (49.70, 51.30) \text{ meV}$ for NH, and $m_1 \in (48.70, 50.30) \text{ meV}$, $m_2 = (49.4, 51.0) \text{ meV}$, $m_3 = 0$ for IH. The sum of neutrino masses are predicted to be

$$\sum m_\nu (\text{meV}) \in \begin{cases} (58.25, 60.25) \text{ for NH,} \\ (98.50, 101.0) \text{ for IH,} \end{cases} \quad (62)$$

which are in consistent with the limits [38] $\sum m_\nu < 0.15 \text{ eV}$ (NH) and $\sum m_\nu < 0.17 \text{ eV}$ (IH), $\sum m_\nu < 0.14 \text{ eV}$ [39], $\sum m_\nu < 0.152 \text{ eV}$ [40] (minimal $\Lambda\text{CDM} + \sum m_\nu$), $\sum m_\nu < 0.118 \text{ eV}$ (high- l polarization), $\sum m_\nu < 0.101 \text{ eV}$ (NPDDE model), $\sum m_\nu < 0.093 \text{ eV}$ (NPDDE+ r model) and the most aggressive bound is $\sum m_\nu < 0.078 \text{ eV}$ (NPDDE+ r with the R16 prior) [40, 41], $\sum m_\nu < 0.183 \text{ eV}$ for IH [42], $\sum m_\nu < 0.13 \text{ eV}$ (the base dataset) and $\sum m_\nu < 0.11 \text{ eV}$ (pol dataset) [43], $\sum m_\nu < 0.19 \text{ eV}$ [44].

In order to determine the possible ranges of the parameters $k_{1,2}, n_{1,2}, t_{1,2}$ and get predictive values for the Dirac CP violation phase δ , we use the observables Δm_{21}^2 , Δm_{31}^2 , $\sin^2 \theta_{12}$, $\sin^2 \theta_{23}$ and $\sin^2 \theta_{13}$, whose experimental values given in Table III, as input parameters.

Table III. The global analysis of neutrino oscillation data [37]

	Best – fit point (3σ range) (NH)	Best – fit point (3σ range) (IH)
Δm_{21}^2 [meV ²]	75.0 (69.4 → 81.4)	75.0 (69.4 → 81.4)
$\frac{ \Delta m_{31}^2 }{10^3}$ [meV ²]	2.55 (2.47 → 2.63)	2.45 (2.37 → 2.53)
$\sin^2 \theta_{12}$	0.318 (0.271 → 0.369)	0.318 (0.271 → 0.369)
$\sin^2 \theta_{23}$	0.574 (0.434 → 0.610)	0.578 (0.433 → 0.608)
$\frac{\sin^2 \theta_{13}}{10^{-2}}$	2.200 (2.00 → 2.405)	2.225 (2.018 → 2.424)
δ_{CP}/π	1.08 (0.71 → 1.99)	1.58 (1.11 → 1.96)

At the best-fit values of the lepton mixing angles[37], $\sin^2 \theta_{12} = 0.318$ and $\sin^2 \theta_{13} = 2.200 \times 10^{-2}$ for NH while $\sin^2 \theta_{12} = 0.318$ and $\sin^2 \theta_{13} = 2.225 \times 10^{-2}$ for IH, $s_\delta, k_{1,2}, n_{1,2}$ and $t_{1,2}$ depend on two parameters c_θ and s_ψ . The Dirac CP violating phase δ (more precisely, s_δ) as a function of two parameters c_θ and s_ψ , with $c_\theta \in (0.29, 0.31)$ and $s_\psi \in (0.25, 0.65)$ for both IH and NH, is plotted in Fig. 3, which implies that

$$s_\delta \in (-0.95, -0.50), \text{ i.e., } \delta^\circ \in (288.20, 330.00) \text{ (NH and IH)}. \quad (63)$$

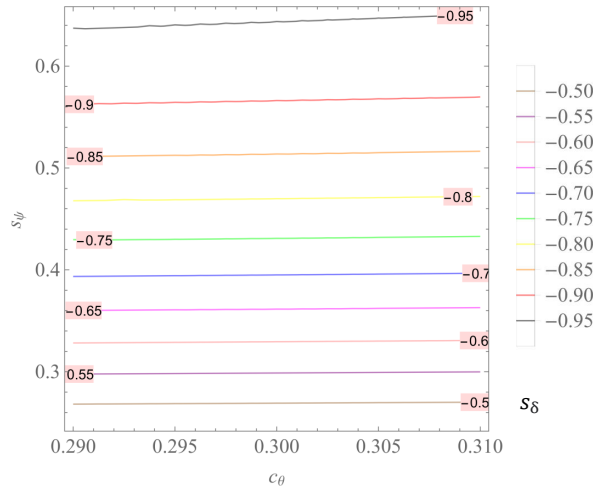


Figure 3. s_δ versus c_θ and s_ψ with $c_\theta \in (0.29, 0.31)$ and $s_\psi \in (0.25, 0.65)$ for both NH and IH.

The dependence of $k_{1,2}$, $n_{1,2}$ and $t_{1,2}$ on two parameters c_θ and s_ψ , with $c_\theta \in (0.29, 0.31)$ and $s_\psi \in (0.25, 0.65)$ for both IH and NH, are respectively plotted in Figs. 4,5, 6,7, 8 and 9.

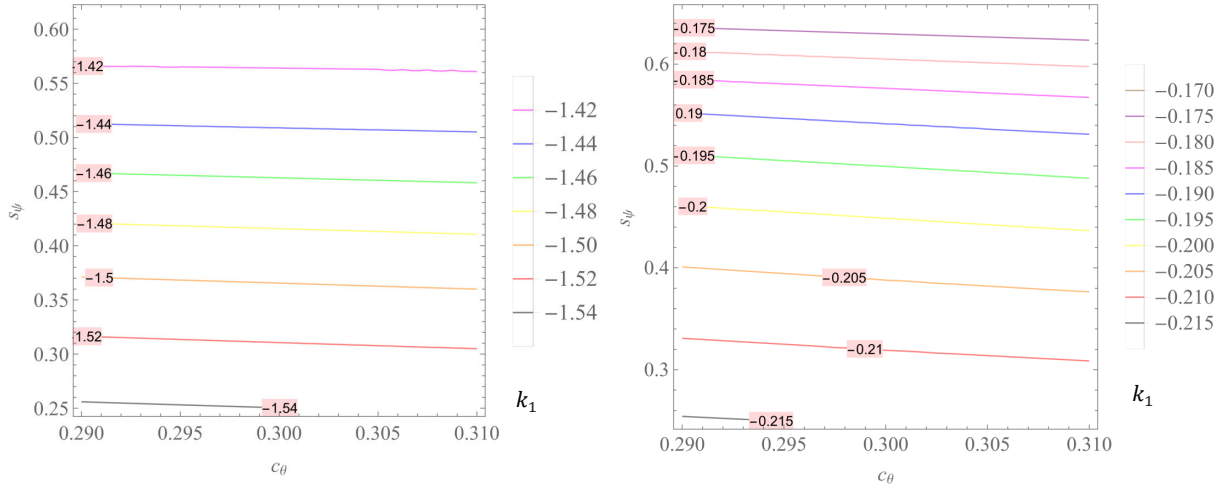


Figure 4. k_1 versus c_θ and s_ψ with $c_\theta \in (0.29, 0.31)$ and $s_\psi \in (0.25, 0.65)$ for NH (left panel) and IH (right panel).

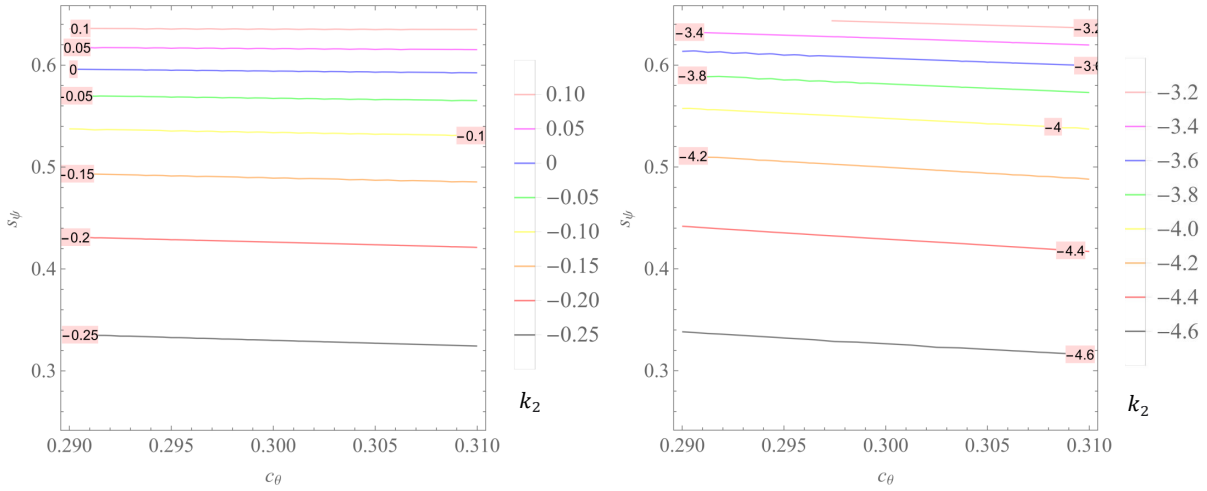


Figure 5. k_2 versus c_θ and s_ψ with $c_\theta \in (0.29, 0.31)$ and $s_\psi \in (0.25, 0.65)$ for NH (left panel) and IH (right panel).

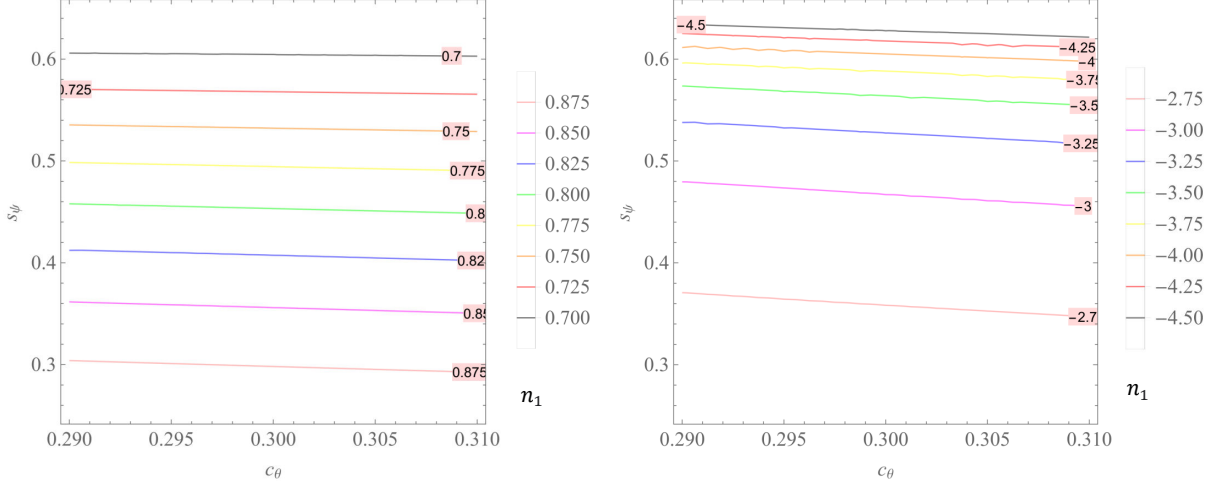


Figure 6. n_1 versus c_θ and s_ψ with $c_\theta \in (0.29, 0.31)$ and $s_\psi \in (0.25, 0.65)$ for NH (left panel) and IH (right panel).

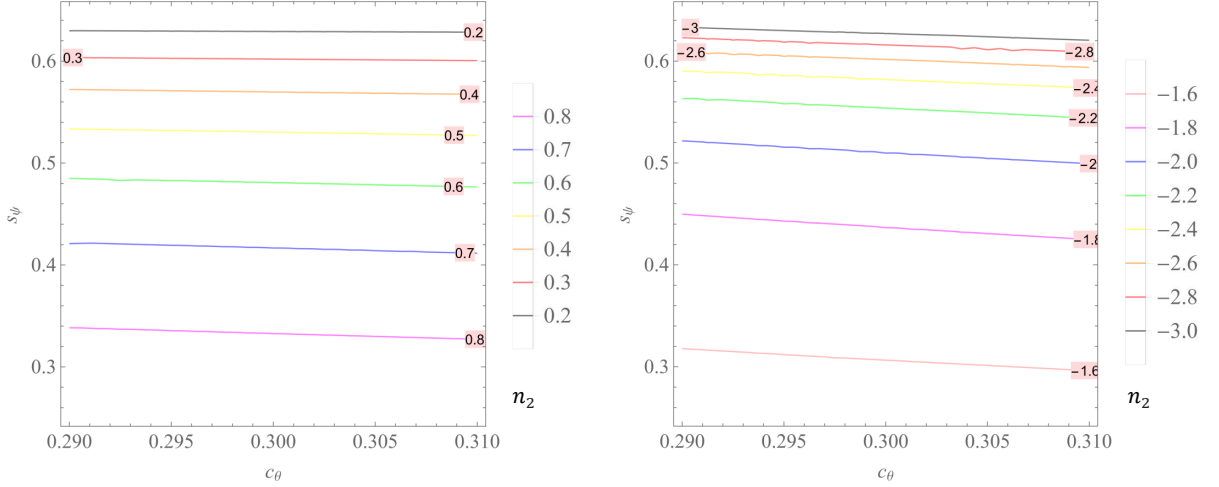


Figure 7. n_2 versus c_θ and s_ψ with $c_\theta \in (0.29, 0.31)$ and $s_\psi \in (0.25, 0.65)$ for NH (left panel) and IH (right panel).

These figures imply:

$$k_1 \in \begin{cases} (-1.54, -1.42) & \text{for NH,} \\ (-0.215, -0.170) & \text{for IH,} \end{cases} \quad k_2 \in \begin{cases} (-0.25, 0.10) & \text{for NH,} \\ (-4.60, -3.20) & \text{for IH,} \end{cases} \quad (64)$$

$$n_1 \in \begin{cases} (0.70, 0.875) & \text{for NH,} \\ (-4.50, -2.75) & \text{for IH,} \end{cases} \quad n_2 \in \begin{cases} (0.20, 0.80) & \text{for NH,} \\ (-3.00, -1.60) & \text{for IH,} \end{cases} \quad (65)$$

$$t_1 \in \begin{cases} (0.30, 1.00) & \text{for NH,} \\ (0.90, 1.20) & \text{for IH,} \end{cases} \quad t_2 \in \begin{cases} (-5.00, -1.50) & \text{for NH,} \\ (-1.50, -0.90) & \text{for IH.} \end{cases} \quad (66)$$

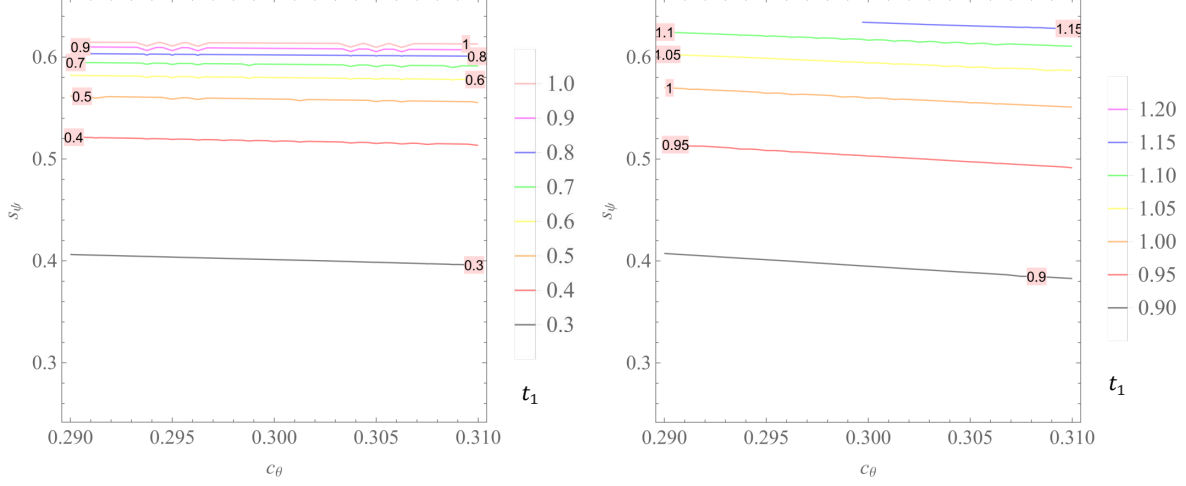


Figure 8. t_1 versus c_θ and s_ψ with $c_\theta \in (0.29, 0.31)$ and $s_\psi \in (0.25, 0.65)$ for NH (left panel) and IH (right panel).

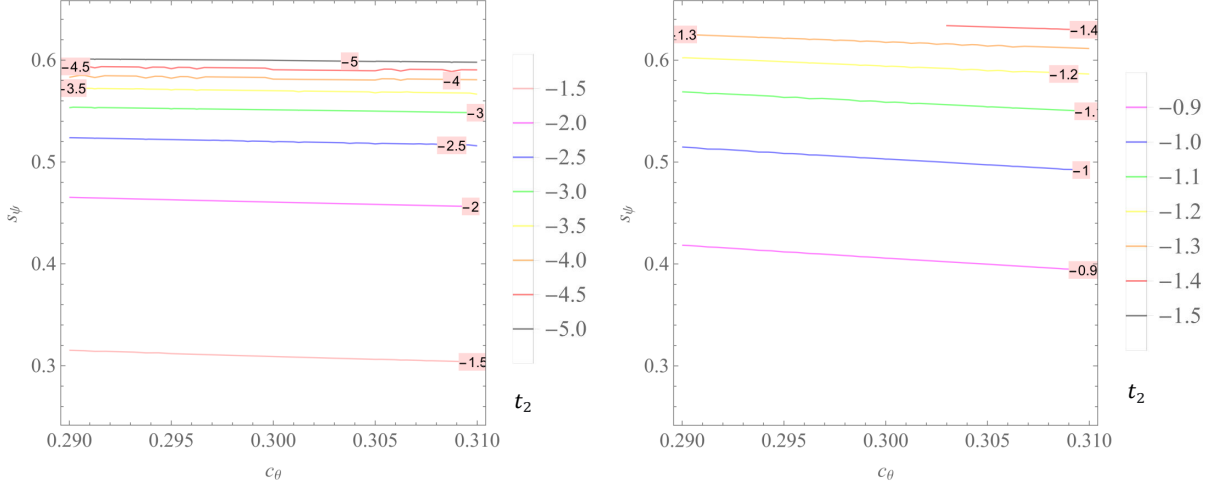


Figure 9. t_2 versus c_θ and s_ψ with $c_\theta \in (0.29, 0.31)$ and $s_\psi \in (0.25, 0.65)$ for NH (left panel) and IH (right panel).

Similarly, to determine the possible ranges of the parameters $A, B_{1,2}, C_{1,2,3}, \langle m_{ee} \rangle$ and m_β we fix $\sin^2 \theta_{12}, \sin^2 \theta_{23}$ and $\sin^2 \theta_{13}$ at their best-fit points [37] and $c_\theta = 0.30$ ($\theta = 72.54^\circ$) and $s_\psi = 0.40$ ($\psi = 23.58^\circ$) for both IH and NH, and Δm_{21}^2 and Δm_{31}^2 take the values in their 3σ ranges [37], $\Delta m_{21}^2 \in (69.4, 81.4) \text{ meV}^2$ and $\Delta m_{31}^2 \in (2.47, 2.63) 10^3 \text{ meV}^2$ (NH) while $\Delta m_{31}^2 \in (-2.53, -2.37) 10^3 \text{ meV}^2$ (IH). The dependence of $A, B_{1,2}, C_{1,2,3}, \langle m_{ee} \rangle$ and m_β on two parameters Δm_{21}^2 and Δm_{31}^2 are presented in Figs. 10, 11, 12, 13, 14, 15, 16 and 17, respectively.

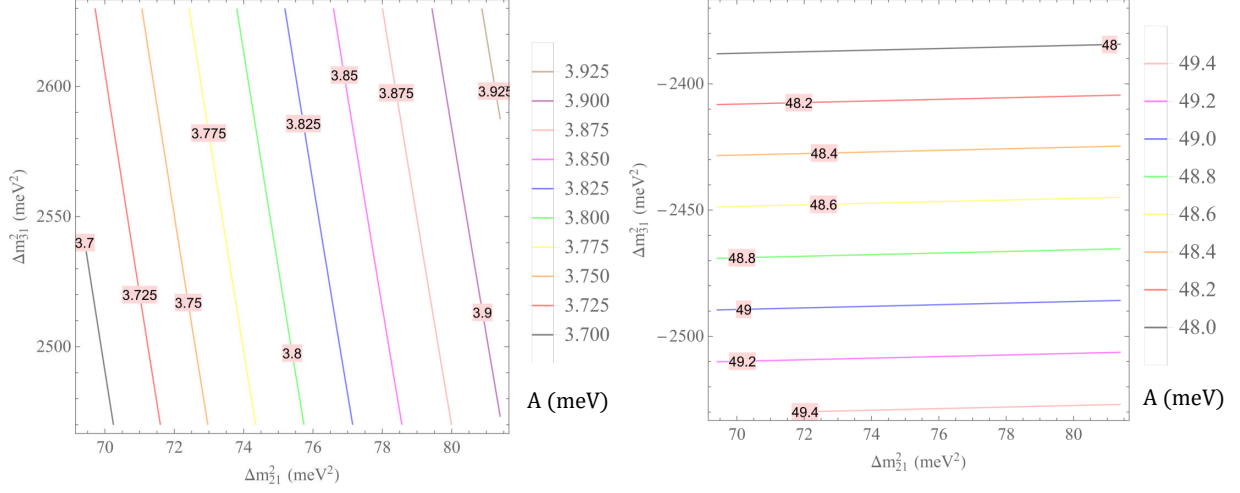


Figure 10. A (meV) versus Δm_{21}^2 and Δm_{31}^2 with $\Delta m_{21}^2 \in (69.4, 81.4) \text{ meV}^2$ and $\Delta m_{31}^2 \in (2.47, 2.63)10^3 \text{ meV}^2$ for NH (left panel) and $\Delta m_{31}^2 \in (-2.53, -2.37)10^3 \text{ meV}^2$ for IH (right panel).

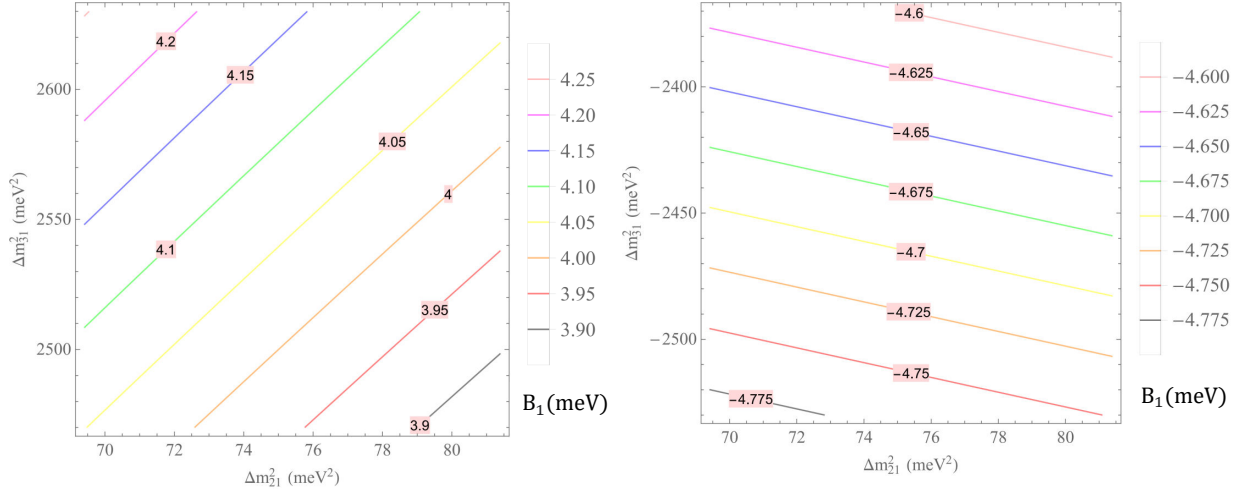


Figure 11. B_1 (meV) versus Δm_{21}^2 and Δm_{31}^2 with $\Delta m_{21}^2 \in (69.4, 81.4) \text{ meV}^2$ and $\Delta m_{31}^2 \in (2.47, 2.63)10^3 \text{ meV}^2$ for NH (left panel) and $\Delta m_{31}^2 \in (-2.53, -2.37)10^3 \text{ meV}^2$ for IH (right panel).

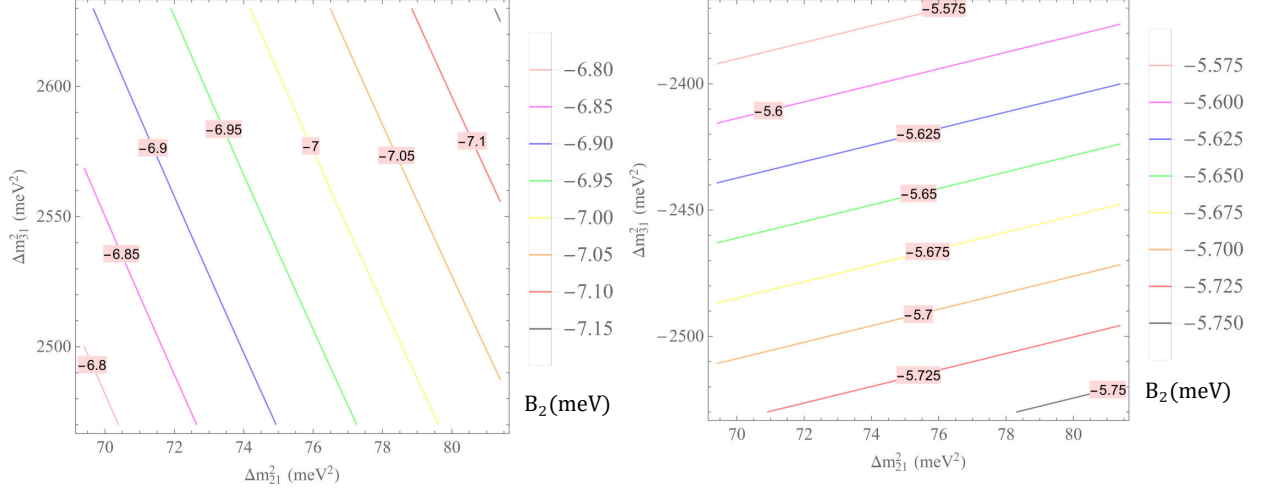


Figure 12. B_2 (meV) versus Δm_{21}^2 and Δm_{31}^2 with $\Delta m_{21}^2 \in (69.4, 81.4) \text{ meV}^2$ and $\Delta m_{31}^2 \in (2.47, 2.63) 10^3 \text{ meV}^2$ for NH (left panel) and $\Delta m_{31}^2 \in (-2.53, -2.37) 10^3 \text{ meV}^2$ for IH (right panel).

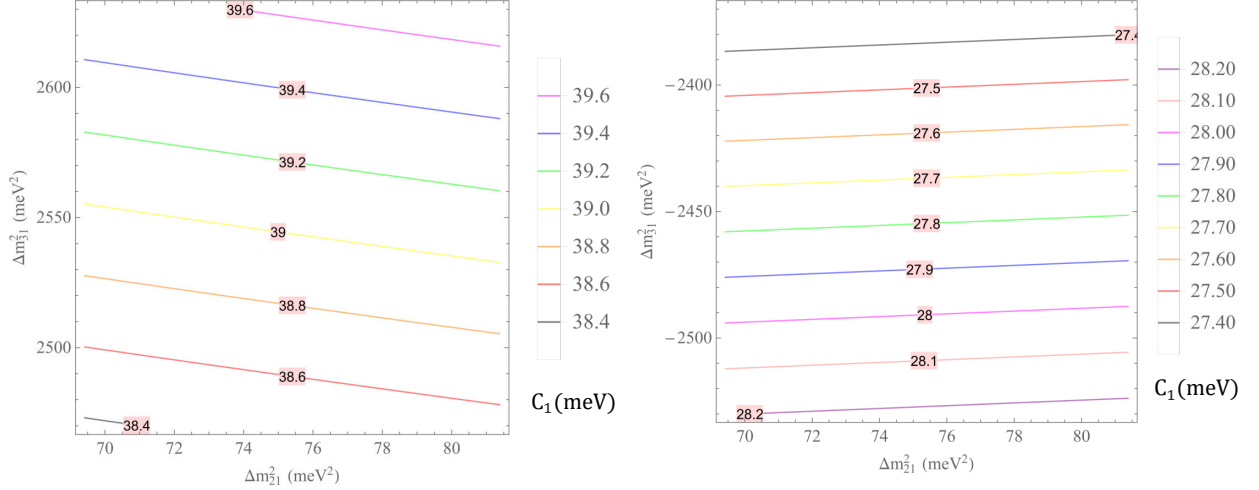


Figure 13. C_1 (meV) versus Δm_{21}^2 and Δm_{31}^2 with $\Delta m_{21}^2 \in (69.4, 81.4) \text{ meV}^2$ and $\Delta m_{31}^2 \in (2.47, 2.63) 10^3 \text{ meV}^2$ for NH (left panel) and $\Delta m_{31}^2 \in (-2.53, -2.37) 10^3 \text{ meV}^2$ for IH (right panel).

Figures 10 and 15 imply that:

$$A \in \begin{cases} (3.700, 3.925) \text{ meV} & \text{for NH,} \\ (48.00, 49.40) \text{ meV} & \text{for IH,} \end{cases} \quad B_1 \in \begin{cases} (3.90, 4.25) \text{ meV} & \text{for NH,} \\ (-4.775, -4.60) \text{ meV} & \text{for IH,} \end{cases} \quad (67)$$

$$B_2 \in \begin{cases} (-7.15, -6.80) \text{ meV} & \text{for NH,} \\ (-5.75, -5.575) \text{ meV} & \text{for IH,} \end{cases} \quad C_1 \in \begin{cases} (38.40, 39.60) \text{ meV} & \text{for NH,} \\ (27.40, 28.20) \text{ meV} & \text{for IH.} \end{cases} \quad (68)$$

$$C_2 \in \begin{cases} (16.00, 16.60) \text{ meV} & \text{for NH,} \\ (23.00, 23.70) \text{ meV} & \text{for IH,} \end{cases} \quad C_3 \in \begin{cases} (-19.00, -18.20) \text{ meV} & \text{for NH,} \\ (-24.70, -24.00) \text{ meV} & \text{for IH.} \end{cases} \quad (69)$$

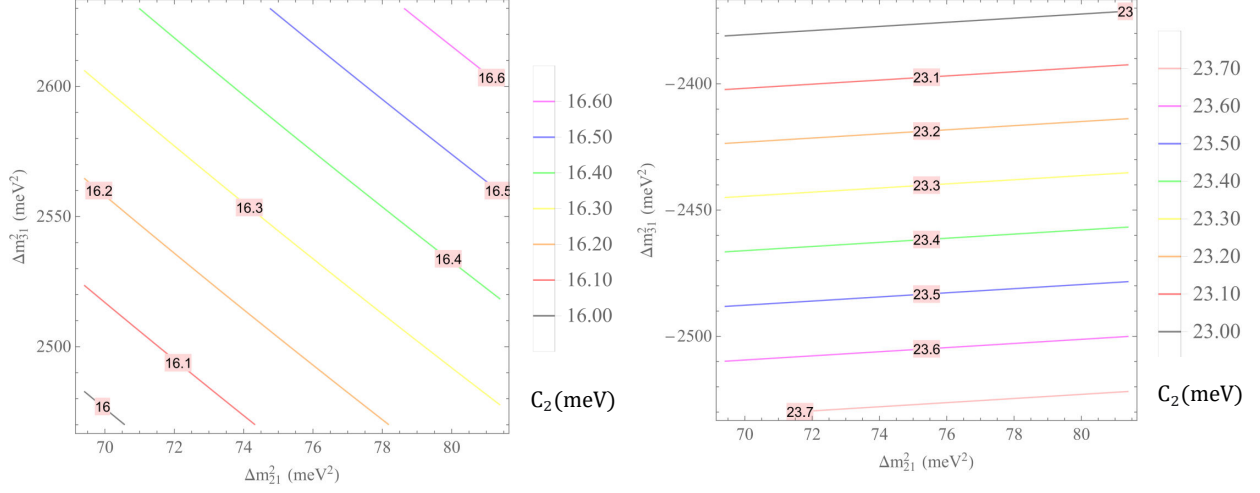


Figure 14. C_2 (meV) versus Δm_{21}^2 and Δm_{31}^2 with $\Delta m_{21}^2 \in (69.4, 81.4) \text{ meV}^2$ and $\Delta m_{31}^2 \in (2.47, 2.63)10^3 \text{ meV}^2$ for NH (left panel) and $\Delta m_{31}^2 \in (-2.53, -2.37)10^3 \text{ meV}^2$ for IH (right panel).

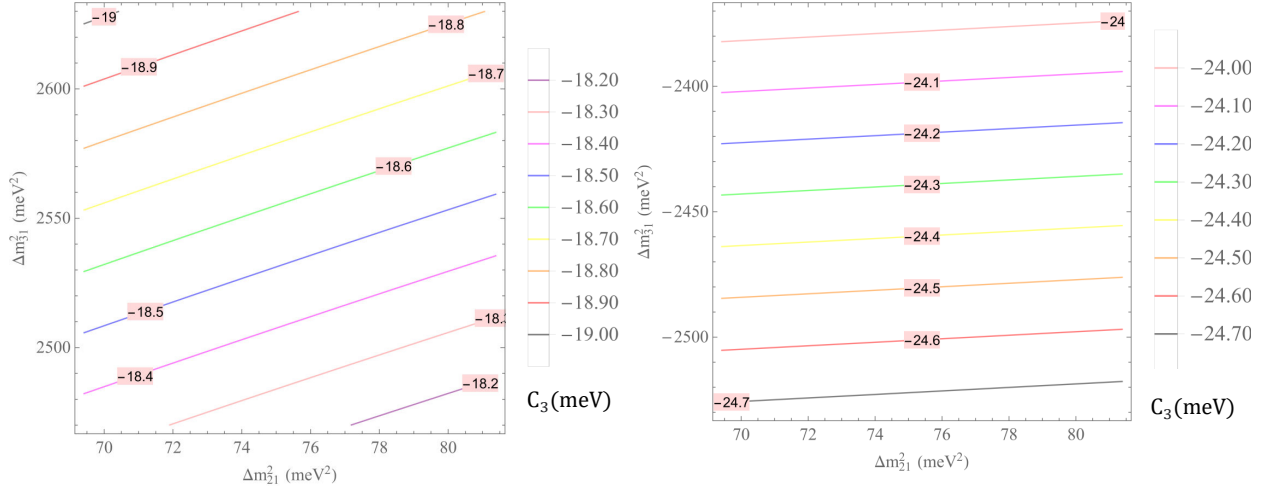


Figure 15. C_3 (meV) versus Δm_{21}^2 and Δm_{31}^2 with $\Delta m_{21}^2 \in (69.4, 81.4) \text{ meV}^2$ and $\Delta m_{31}^2 \in (2.47, 2.63)10^3 \text{ meV}^2$ for NH (left panel) and $\Delta m_{31}^2 \in (-2.53, -2.37)10^3 \text{ meV}^2$ for IH (right panel).

Figures 16 and 17 show the predictive regions of the effective neutrino-masses:

$$\langle m_{ee} \rangle \in \begin{cases} (3.700, 3.925) \text{ meV} & \text{for NH,} \\ (48.00, 49.40) \text{ meV} & \text{for IH,} \end{cases} \quad m_\beta \in \begin{cases} (8.75, 9.10) \text{ meV} & \text{for NH,} \\ (48.40, 49.80) \text{ meV} & \text{for IH,} \end{cases} \quad (70)$$

which are below the upper limits for $\langle m_{ee} \rangle$ from KamLAND-Zen [45] $\langle m_{ee} \rangle < 61 \div 165 \text{ meV}$, GERDA [46] $\langle m_{ee} \rangle < 104 \div 228 \text{ meV}$ and CUORE [47] $\langle m_{ee} \rangle < 75 \div 350 \text{ meV}$, and the constraints for m_β with $8.5 \text{ meV} < m_\beta < 1.1 \text{ eV}$ for NH and $48 \text{ meV} < m_\beta < 1.1 \text{ eV}$ for IH [1], $m_\beta \in (8.90 \div 12.60) \text{ eV}$ [48], and $m_\beta < 0.8 \text{ eV}$ [49].

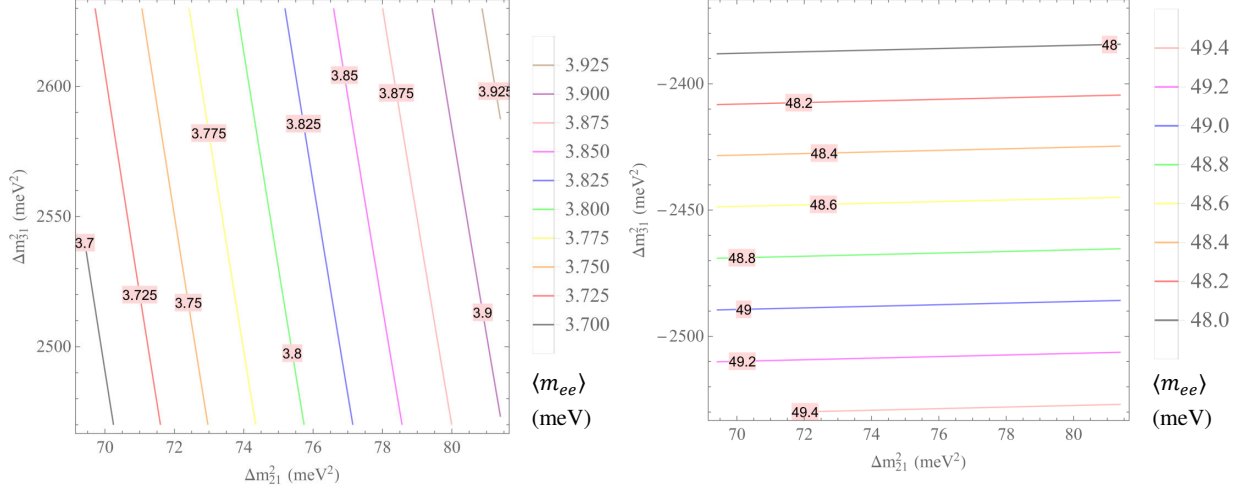


Figure 16. $\langle m_{ee} \rangle$ (meV) versus Δm_{21}^2 and Δm_{31}^2 with $\Delta m_{21}^2 \in (69.4, 81.4) \text{ meV}^2$ and $\Delta m_{31}^2 \in (2.47, 2.63) 10^3 \text{ meV}^2$ for NH (left panel) and $\Delta m_{31}^2 \in (-2.53, -2.37) 10^3 \text{ meV}^2$ for IH (right panel).

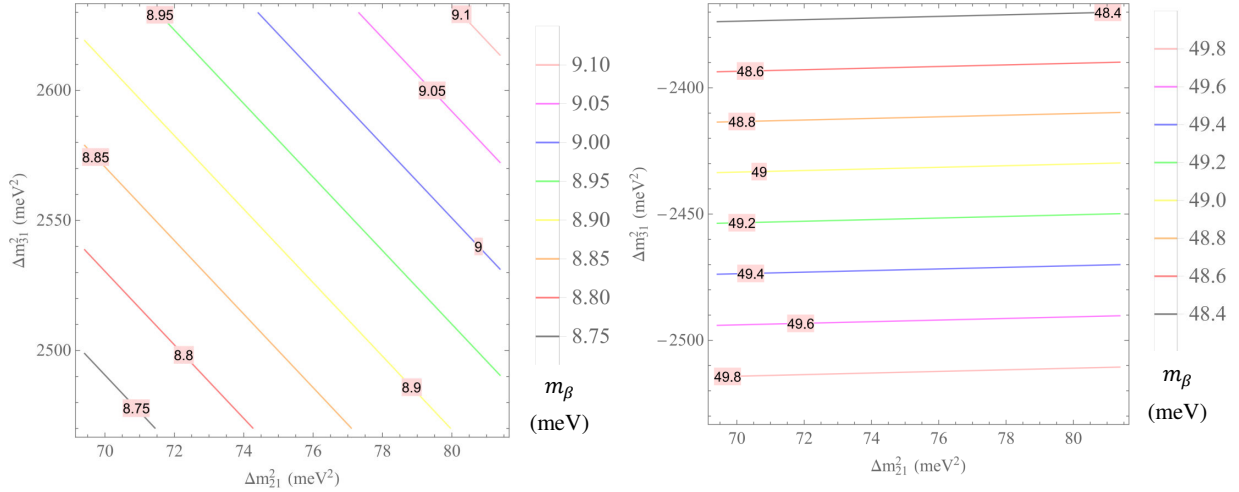


Figure 17. m_β (meV) versus Δm_{21}^2 and Δm_{31}^2 with $\Delta m_{21}^2 \in (69.4, 81.4) \text{ meV}^2$ and $\Delta m_{31}^2 \in (2.47, 2.63) 10^3 \text{ meV}^2$ for NH (left panel) and $\Delta m_{31}^2 \in (-2.53, -2.37) 10^3 \text{ meV}^2$ for IH (right panel).

VI. CONCLUSIONS

We have constructed a gauge $B - L$ model with $D_4 \times Z_4 \times Z_2$ symmetry that can explain the quark and lepton mass hierarchies and their mixing patterns with the realistic CP phases via the type-I seesaw mechanism. Six quark masses, three quark mixing angles and CP phase in the quark sector can get the central values and Yukawa couplings in the quark sector are diluted a range of three orders of magnitude difference by the perturbation theory at the first order. For neutrino sector, the smallness of neutrino mass is achieved by the Type-I seesaw mechanism.

Both inverted and normal neutrino mass hierarchies are in consistent with the experimental data. The prediction for the sum of neutrino masses is $58.25\text{meV} \leq \sum m_\nu \leq 60.25 \text{ meV}$ for normal hierarchy and $98.50\text{meV} \leq \sum m_\nu \leq 101.00 \text{ meV}$ for inverted hierarchy which are well consistent with all the recent limits. In addition, the Dirac CP phase is predicted to be $288.20 \leq \delta(^{\circ}) \leq 330.00$ within the 3σ range of experimental constraint. The effective neutrino masses are predicted to be $3.700\text{meV} \leq \langle m_{ee} \rangle \leq 3.925 \text{ meV}$, $8.75\text{meV} \leq m_\beta \leq 9.10\text{meV}$ for normal hierarchy and $48.00\text{meV} \leq \langle m_{ee} \rangle \leq 49.40 \text{ meV}$ and $48.40\text{meV} \leq m_\beta \leq 49.80\text{meV}$ for inverted hierarchy which are in consistence with the recent constraints.

ACKNOWLEDGMENTS

This research is funded by Tay Nguyen University under grant number T2023-45CBTĐ.

Appendix A: Forbidden terms under the model's symmetries

Table IV. Yukawa terms forbidden by the model's symmetries

Yukawa terms	Forbidden by
$ \begin{aligned} & (\bar{\psi}_{\alpha L} l_{\alpha R})_{1+-} \tilde{H}, (\bar{\psi}_{\alpha L} l_{\alpha R})_{1-+} \tilde{H}'; (\bar{\psi}_{1L} \nu_{\alpha R})_2 (H \rho^*)_2, (\bar{\psi}_{1L} \nu_{\alpha R})_2 (H' \rho^*)_2; \\ & (\bar{\psi}_{\alpha L} \nu_{\alpha R})_{1-+} (\tilde{H} \varphi)_{1-+}, (\bar{\psi}_{\alpha L} \nu_{\alpha R})_{1+-} (\tilde{H}' \varphi)_{1+-}; (Q_{1L} u_{1R})_{1++} (H \phi)_{1++}, \\ & (Q_{\alpha L} u_{\alpha R})_{1++} (H \phi)_{1++}, (Q_{\alpha L} u_{\alpha R})_{1+-} H, (Q_{\alpha L} u_{\alpha R})_{1-+} H', (Q_{\alpha L} u_{\alpha R})_{1--} (H' \phi)_{1--}; \\ & (Q_{1L} u_{\alpha R})_2 (H \rho)_2, (Q_{1L} u_{\alpha R})_2 (H' \rho)_2, (Q_{\alpha L} u_{1R})_2 (H \rho^*)_2, (Q_{\alpha L} u_{1R})_2 (H' \rho^*)_2, \\ & (Q_{1L} d_{1R})_{1++} (\tilde{H} \phi)_{1++}, (Q_{\alpha L} d_{\alpha R})_{1++} (\tilde{H} \phi)_{1++}, (Q_{\alpha L} d_{\alpha R})_{1+-} \tilde{H}, (Q_{\alpha L} d_{\alpha R})_{1-+} \tilde{H}', \\ & (Q_{\alpha L} d_{\alpha R})_{1--} (\tilde{H}' \phi)_{1--}; (Q_{1L} d_{\alpha R})_2 (\tilde{H} \rho)_2, (Q_{1L} d_{\alpha R})_2 (\tilde{H}' \rho)_2, \\ & (Q_{\alpha L} d_{1R})_2 (\tilde{H} \rho^*)_2, (Q_{\alpha L} d_{1R})_2 (\tilde{H}' \rho^*)_2 \end{aligned} $	$U(1)_Y$
$ \begin{aligned} & (\bar{\nu}_{1R}^C \nu_{1R})_{1++} (\phi \chi^*)_{1++}, (\bar{\nu}_{1R}^C \nu_{1R})_{1++} (\rho^2)_{1++}, (\bar{\nu}_{1R}^C \nu_{1R})_{1++} (\rho^{*2})_{1++}; \\ & (\bar{\nu}_{\alpha R}^C \nu_{\alpha R})_{1++} (\phi \chi^*)_{1++}, (\bar{\nu}_{\alpha R}^C \nu_{\alpha R})_{1++} (\rho^2)_{1++}, (\bar{\nu}_{\alpha R}^C \nu_{\alpha R})_{1++} (\rho^{*2})_{1++}; \\ & (\bar{\nu}_{\alpha R}^C \nu_{\alpha R})_{1+-} \chi^*; (\bar{\psi}_{1L} \psi_{1L}^C)_{1++} \tilde{H}^2, (\bar{\psi}_{1L} \psi_{1L}^C)_{1++} \tilde{H}^2. \end{aligned} $	$U(1)_{B-L}$
$ \begin{aligned} & (\bar{\psi}_{1L} l_{1R})_{1++} H, (\bar{\psi}_{1L} l_{1R})_{1++} H', (\bar{\psi}_{1L} l_{1R})_{1++} (H' \phi)_{1--}; (\bar{\psi}_{1L} \nu_{1R})_{1+-} (H \rho^*)_2, \\ & (\bar{\psi}_{1L} \nu_{1R})_{1+-} (H' \rho^*)_2; (\bar{\psi}_{\alpha L} \nu_{1R})_2 (\tilde{H} \varphi)_{1-+}, (\bar{\psi}_{\alpha L} \nu_{1R})_2 (\tilde{H}' \varphi)_{1-+}; (\bar{\nu}_{1R}^C \nu_{1R})_{1++} \chi; \\ & (\bar{\nu}_{1R}^C \nu_{\alpha R})_2 \chi, (\bar{\nu}_{1R}^C \nu_{\alpha R})_2 (\phi \chi)_{1++}; (Q_{1L} u_{1R})_{1++} \tilde{H}, (Q_{1L} u_{1R})_{1++} \tilde{H}', \\ & (Q_{1L} u_{1R})_{1++} (\tilde{H}' \phi)_{1--}, (Q_{\alpha L} u_{\alpha R})_{1++} \tilde{H}, (Q_{\alpha L} u_{\alpha R})_{1++} \tilde{H}', (Q_{\alpha L} u_{\alpha R})_{1++} (\tilde{H}' \phi)_{1--}, \\ & (Q_{1L} d_{1R})_{1++} H, (Q_{1L} d_{1R})_{1++} H', (Q_{1L} d_{1R})_{1++} (H' \phi)_{1--}, \\ & (Q_{\alpha L} d_{\alpha R})_{1++} H, (Q_{\alpha L} d_{\alpha R})_{1++} H', (Q_{\alpha L} d_{\alpha R})_{1++} (H' \phi)_{1--} \end{aligned} $	D_4
$ \begin{aligned} & (\bar{\psi}_{1L} \nu_{\alpha R})_2 (\tilde{H} \rho)_2, (\bar{\psi}_{1L} \nu_{\alpha R})_2 (\tilde{H}' \rho)_2, (\bar{\psi}_{\alpha L} \nu_{1R})_2 (\tilde{H} \rho)_2, (\bar{\psi}_{\alpha L} \nu_{1R})_2 (\tilde{H} \rho^*)_2, \\ & (\bar{\psi}_{\alpha L} \nu_{1R})_2 (\tilde{H}' \rho)_2, (\bar{\psi}_{\alpha L} \nu_{1R})_2 (\tilde{H}' \rho^*)_2, (Q_{1L} u_{\alpha R})_2 (H \rho^*)_2, (Q_{1L} u_{\alpha R})_2 (H' \rho^*)_2, \\ & (Q_{\alpha L} u_{1R})_2 (H \rho)_2, (Q_{\alpha L} u_{1R})_2 (H' \rho)_2; (Q_{1L} d_{\alpha R})_2 (\tilde{H} \rho^*)_2, (Q_{1L} d_{\alpha R})_2 (\tilde{H}' \rho^*)_2, \\ & (Q_{\alpha L} d_{1R})_2 (\tilde{H} \rho)_2, (Q_{\alpha L} d_{1R})_2 (\tilde{H}' \rho)_2 \end{aligned} $	Z_4
$ \begin{aligned} & (\bar{\psi}_{1L} l_{\alpha R})_2 (H \rho)_2, (\bar{\psi}_{1L} l_{\alpha R})_2 (H' \rho)_2, (\bar{\psi}_{\alpha L} l_{1R})_2 (H \rho^*)_2, (\bar{\psi}_{\alpha L} l_{1R})_2 (H' \rho^*)_2 \end{aligned} $	Z_2

Appendix B: The explicit expressions of $a_{1u,d}$, $a_{2u,d}$, $a_{3u,d}$, $b_{u,d}$, $c_{1u,d}$, $c_{2u,d}$, c_{3u} and $c_{4u,d}$ as functions of quark masses and quark mixing matrix elements

The explicit expressions of $a_{1u,d}$, $a_{2u,d}$, $a_{3u,d}$, $b_{u,d}$, $c_{1u,d}$, $c_{2u,d}$, c_{3u} and $c_{4u,d}$ are:

$$\begin{aligned}
a_{1u} &= m_u, \quad a_{2u} = \frac{m_c + m_t}{2}, \quad a_{3u} = \frac{m_c - m_t}{2}, \\
a_{1d} &= m_d, \quad a_{2d} = \frac{m_s + m_b}{2}, \quad a_{3d} = \frac{m_s - m_b}{2}, \\
c_{1u} &= -c_{3u} + \frac{(m_d - m_s)(m_c - m_u)(1 - V_{11}^{\text{exp}})}{2c_{1d}^*}, \\
c_{2u} &= \frac{(m_u - m_c)(m_d - m_s)}{c_{2d}^* + c_{4d}^*} \left[\frac{4b_d^* b_u}{(m_b - m_s)(m_c - m_t)} + \frac{c_{4u}(c_{2d}^* + c_{4d}^*)}{(m_c - m_u)(m_d - m_s)} + V_{22}^{\text{exp}} - 1 \right], \\
c_{3u} &= \frac{m_u - m_t}{2} \left[\frac{(V_{11}^{\text{exp}} - 1)(m_c - m_u)(m_d - m_s)}{2c_{1d}^*(m_t - m_u)} + \frac{c_{2d}^* - c_{4d}^*}{m_b - m_d} + V_{13}^{\text{exp}} \right], \\
2c_{4u} &= \frac{4b_d^* b_u (m_c - m_u)(m_s - m_d)}{(c_{2d}^* + c_{4d}^*)(m_b - m_s)(m_c - m_t)} - \frac{V_{33}^{\text{exp}}(m_b - m_d)(m_t - m_u)}{c_{2d}^* - c_{4d}^*} \\
&\quad + \frac{(m_b - m_d)(m_t - m_u)}{c_{2d}^* - c_{4d}^*} + \frac{V_{22}^{\text{exp}}(m_u - m_c)(m_d - m_s)}{c_{2d}^* + c_{4d}^*} + \frac{(m_c - m_u)(m_d - m_s)}{c_{2d}^* + c_{4d}^*}, \quad (\text{B1}) \\
b_u &= \frac{(m_b - m_s)(m_c - m_t) \{ (c_{2d}^* + c_{4d}^*) [2c_{1d}^* + (m_d - m_s)V_{21}^{\text{exp}}] + (m_d - m_s)^2 (1 - V_{22}^{\text{exp}}) \}}{4b_d^*(m_d - m_s)^2}, \\
b_d^* &= \frac{(m_b - m_d)(m_b - m_s) \{ (1 - V_{11}^{\text{exp}})(m_d - m_s)^2 + 2c_{1d}^* [c_{2d}^* + c_{4d}^* + (m_s - m_d)V_{12}^{\text{exp}}] \}}{4c_{1d}^*(m_d - m_s) [c_{4d}^* - c_{2d}^* + V_{13}^{\text{exp}}(m_d - m_b)]}, \\
c_{2d}^* &= \frac{c_{4d}^* V_{31}^{\text{exp}} + (V_{33}^{\text{exp}} - 1)(m_d - m_b)}{V_{31}^{\text{exp}}}, \quad c_{4d}^* = \{ 2c_{1d}^*(m_d - m_s) [m_b \mathbf{F}_q + m_d \mathbf{G}_q + m_s \mathbf{H}_q] \\
&\quad + (m_d - m_s)^3 \mathbf{T}_q + 4c_{1d}^{*2} (V_{33}^{\text{exp}} - 1) [V_{13}^{\text{exp}}(m_b - m_d) + V_{12}^{\text{exp}}(m_d - m_s)] \} / \{ 4c_{1d}^* V_{31}^{\text{exp}} [2c_{1d}^* V_{13}^{\text{exp}} \\
&\quad + (m_d - m_s)(V_{13}^{\text{exp}} V_{21}^{\text{exp}} - V_{23}^{\text{exp}})] \}, \\
c_{1d}^* &= \frac{(m_s - m_d) \sqrt{\mathbf{K}_{1q}} + (m_s - m_d) \mathbf{P}_{1q} + V_{13}^{\text{exp}}(m_d - m_s) [(V_{22}^{\text{exp}} - 1)V_{31}^{\text{exp}} - V_{21}^{\text{exp}} V_{32}^{\text{exp}}]}{4V_{13}^{\text{exp}} V_{32}^{\text{exp}} - 4V_{12}^{\text{exp}} V_{33}^{\text{exp}}},
\end{aligned}$$

where

$$\begin{aligned}
\mathbf{F}_q &= (V_{33}^{\text{exp}} - 1)(V_{13}^{\text{exp}} V_{21}^{\text{exp}} - V_{23}^{\text{exp}}), \quad \mathbf{G}_q = V_{33}^{\text{exp}} [V_{11}^{\text{exp}} + (V_{12}^{\text{exp}} - V_{13}^{\text{exp}})V_{21}^{\text{exp}} - V_{22}^{\text{exp}} + V_{23}^{\text{exp}}] \\
&\quad + V_{22}^{\text{exp}} - V_{23}^{\text{exp}} - V_{11}^{\text{exp}} - V_{12}^{\text{exp}}(V_{21}^{\text{exp}} + V_{23}^{\text{exp}} V_{31}^{\text{exp}}) + V_{13}^{\text{exp}} [V_{21}^{\text{exp}} + (V_{22}^{\text{exp}} - 1)V_{31}^{\text{exp}}], \\
\mathbf{H}_q &= (V_{11}^{\text{exp}} + V_{22}^{\text{exp}})(1 - V_{33}^{\text{exp}}) + V_{12}^{\text{exp}}(V_{21}^{\text{exp}} - V_{21}^{\text{exp}} V_{33}^{\text{exp}} + V_{23}^{\text{exp}} V_{31}^{\text{exp}}) + V_{13}^{\text{exp}} V_{31}^{\text{exp}}(1 - V_{22}^{\text{exp}}), \\
\mathbf{T}_q &= (1 - V_{11}^{\text{exp}}) [V_{21}^{\text{exp}}(1 - V_{33}^{\text{exp}}) + V_{23}^{\text{exp}} V_{31}^{\text{exp}}], \quad (\text{B2}) \\
\mathbf{K}_{1q} &= [(V_{11}^{\text{exp}} + V_{12}^{\text{exp}} V_{21}^{\text{exp}}) V_{33}^{\text{exp}} - V_{12}^{\text{exp}} V_{23}^{\text{exp}} V_{31}^{\text{exp}} - V_{13}^{\text{exp}} V_{21}^{\text{exp}} V_{32}^{\text{exp}} + (V_{22}^{\text{exp}} - 1) V_{13}^{\text{exp}} V_{31}^{\text{exp}} \\
&\quad - V_{22}^{\text{exp}} V_{33}^{\text{exp}} + V_{23}^{\text{exp}} V_{32}^{\text{exp}}]^2 + 4(V_{11}^{\text{exp}} - 1)(V_{13}^{\text{exp}} V_{32}^{\text{exp}} - V_{12}^{\text{exp}} V_{33}^{\text{exp}})(V_{21}^{\text{exp}} V_{33}^{\text{exp}} - V_{23}^{\text{exp}} V_{31}^{\text{exp}}), \\
\mathbf{P}_{1q} &= (V_{22}^{\text{exp}} - V_{11}^{\text{exp}} - V_{12}^{\text{exp}} V_{21}^{\text{exp}}) V_{33}^{\text{exp}} + (V_{12}^{\text{exp}} V_{31}^{\text{exp}} - V_{32}^{\text{exp}}) V_{23}^{\text{exp}}.
\end{aligned}$$

Appendix C: The explicit expressions of $k_{1,2}$, $n_{1,2}$ and $t_{1,2}$ as functions of

$a_D, b_D, c_D, f_D, g_D, a_R, b_R$ and c_R

The explicit expressions of $k_{1,2}$, $n_{1,2}$ and $t_{1,2}$ are:

$$k_1 = \frac{c_D - d_D}{a_D + b_D}, \quad k_2 = \frac{a_D - b_D}{c_D + d_D}, \quad (\text{C1})$$

$$n_1 = \left\{ a_D^2 (b_D - a_D) (b_R + c_R) - b_D [(c_R - b_R) (b_D^2 + 2c_D d_D) + (c_D^2 + d_D^2) c_R] \right. \\ \left. - a_D [b_D^2 (b_R - c_R) + 2c_D d_D (b_R + c_R) + (c_D^2 + d_D^2) c_R] + (a_D - b_D) \sqrt{\Delta} \right\} \\ / \left\{ (c_D - d_D) \{ b_D^2 (c_R - b_R) + a_D^2 (b_R + c_R) + [(c_D + d_D)^2 - 2a_D b_D] c_R \} \right\}, \quad (\text{C2})$$

$$n_2 = \left\{ (c_D + d_D) \{ [(a_D + b_D)^2 + (c_D - d_D)^2] c_R^2 + (a_D^2 - b_D^2) c_R b_R + 2(c_D d_D - a_D b_D) b_R^2 \right. \\ \left. - b_R \sqrt{\Delta} \right\} / \left\{ (c_D - d_D) [b_D^2 b_R (c_R - b_R) + a_D^2 b_R (b_R + c_R) + b_R c_R (c_D^2 + d_D^2) - c_R \sqrt{\Delta}] \right\}, \quad (\text{C3})$$

$$t_1 = \left\{ a_D^2 (b_D - a_D) (b_R + c_R) + b_D [(b_D^2 + 2c_D d_D) (b_R - c_R) - (c_D^2 + d_D^2) c_R] \right. \\ \left. - a_D [b_D^2 (b_R - c_R) + c_D^2 c_R + 2c_D d_D (b_R + c_R) + c_R d_D^2] + (b_D - a_D) \sqrt{\Delta} \right\} \\ / \left\{ (c_D - d_D) [b_D^2 (c_R - b_R) - 2a_D b_D c_R + a_D^2 (b_R + c_R) + c_R (c_D + d_D)^2] \right\}, \quad (\text{C4})$$

$$t_2 = \left\{ (c_D + d_D) \{ [(a_D + b_D)^2 + (c_D - d_D)^2] c_R^2 + (a_D^2 - b_D^2) c_R b_R + 2(c_D d_D - a_D b_D) b_R^2 \right. \\ \left. + b_R \sqrt{\Delta} \right\} / \left\{ (c_D - d_D) [b_D^2 b_R (c_R - b_R) + a_D^2 b_R (b_R + c_R) + b_R c_R (c_D^2 + d_D^2) + c_R \sqrt{\Delta}] \right\}, \quad (\text{C5})$$

where

$$\Delta = a_D^4 (b_R + c_R)^2 + [b_D^2 b_R - (b_D^2 + c_D^2) c_R]^2 + 8a_D b_D c_D d_D (c_R^2 - b_R^2) + c_R^2 d_D^4 \\ + 2[2b_R^2 c_D^2 - b_D^2 b_R c_R + (b_D^2 - c_D^2) c_R^2] d_D^2 + 2a_D^2 (b_R + c_R) [b_D^2 (b_R - c_R) + c_R (c_D^2 + d_D^2)]. \quad (\text{C6})$$

-
- [1] R.L. Workman *et al.* (Particle Data Group), *The Review of Particle Physics*, Prog.Theor.Exp.Phys.2022, 083C01 (2022). <https://doi.org/10.1093/ptep/ptac097>.
- [2] A. Davidson, *B – L as the fourth color within an $SU(2)_L \times U(1)_R \times U(1)$ model*, Phys. Rev. D 20, 776 (1979). <https://doi.org/10.1103/PhysRevD.20.776>.
- [3] N. Sahu and U. A. Yajnik, *Dark matter and leptogenesis in gauged B – L symmetric models embedding ν MSM*, Phys. Lett. B 635, 11 (2006). <https://doi.org/10.1016/j.physletb.2006.02.040>.
- [4] S. Khalil, *Low scale B-L extension of the Standard Model at the LHC*, J.Phys.G 35 (2008) 055001. <https://doi.org/10.1088/0954-3899/35/5/055001>.
- [5] P. S. B. Dev, R. N. Mohapatra, Y. Zhang, *Leptogenesis constraints on B-L breaking Higgs boson in TeV scale seesaw models*, J. High Energ. Phys. 2018, 122 (2018). [https://doi.org/10.1007/JHEP03\(2018\)122](https://doi.org/10.1007/JHEP03(2018)122).
- [6] F. F. Deppisch, W. Liu and M. Mitra, *Long-lived heavy neutrinos from Higgs decays*, J. High Energ. Phys. 2018, 181 (2018). [https://doi.org/10.1007/JHEP08\(2018\)181](https://doi.org/10.1007/JHEP08(2018)181).
- [7] T. Hasegawa, N. Okada and O. Seto, *Gravitational waves from the minimal gauged $U(1)_{B-L}$ model*, Phys. Rev. D 99 (2019) 095039. <https://doi.org/10.1103/PhysRevD.99.095039>.
- [8] Jin-Lei Yang, Tai-Fu Feng, Hai-Bin Zhang, *Electron and muon $(g - 2)$ in the B – LSSM*, J. Phys. G: Nucl. Part. Phys. 47 (2020) 055004. <https://doi.org/10.1088/1361-6471/ab7986>.
- [9] V. V. Vien, *B – L extension of the standard model with Q_6 symmetry*, Nucl. Phys. B 956 (2020) 115015. <https://doi.org/10.1016/j.nuclphysb.2020.115015>.
- [10] W. Grimus and L. Lavoura, *A discrete symmetry group for maximal atmospheric neutrino mixing*, Phys. Lett. B 572 (2003) 189. <https://doi.org/10.1016/j.physletb.2003.08.032>.
- [11] W. Grimus, A.S. Joshipura, S. Kaneko, L. Lavoura, M. Tanimoto, *Lepton mixing angle $\theta_{13} = 0$ with a horizontal symmetry D_4* , JHEP 07 (2004) 078. <https://doi.org/10.1088/1126-6708/2004/07/078>.
- [12] A. Adulpravitchai, A. Blum, C. Hagedorn, *A Supersymmetric D_4 Model for mu-tau Symmetry*, JHEP 03 (2009) 046. <https://doi.org/10.1088/1126-6708/2009/03/046>.
- [13] V. V. Vien, H. N. Long, D. P. Khoi, *Type-I seesaw mechanism for neutrino mass and mixing in gauged B-L model with $D_4 \times Z_4$ flavor symmetry*, Mod. Phys. Lett. A 36 (2021) 2150184. <https://doi.org/10.1142/S0217732321501844>.
- [14] C. Hagedorn and R. Ziegler, *$\mu - \tau$ Symmetry and Charged Lepton Mass Hierarchy in a Supersymmetric D_4 Model*, Phys. Rev. D 82 (2010) 053011. <https://doi.org/10.1103/PhysRevD.82.053011>.
- [15] V. V. Vien, *Neutrino mass and mixing in the 3-3-1 model with neutral leptons based on D_4 flavor symmetry*, Mod. Phys. Lett. A 29 (2014) 1450122. <https://doi.org/10.1142/S0217732314501223>.
- [16] V. V. Vien, *Fermion mass and mixing in the $U(1)_{B-L}$ extension of the standard model with D_4 symmetry*, J. Phys. G: Nucl. Part. Phys. 47 (2020) 055007. <https://doi.org/10.1088/1361-6471/ab7ec0>.
- [17] D. Meloni, S. Morisi, and E. Peinado, *Stability of dark matter from the $D_4 \times Z_2$ flavor group*, Phys. Lett. B 703 (2011) 281. <https://doi.org/10.1016/j.physletb.2011.07.084>.

- [18] V. V. Vien and H. N. Long, *The D_4 flavor symmetry in 3-3-1 model with neutral leptons*, Int. J. Mod. Phys. A 28 (2013) 1350159. <https://doi.org/10.1142/S0217751X13501595>.
- [19] V. V. Vien and H. N. Long, *Quark mass and mixing in the 3-3-1 model with neutral leptons based on D_4 flavor symmetry*, J. Korean Phys. Soc. 66 (2015) 1809. <https://doi.org/10.3938/jkps.66.1809>.
- [20] D. Das, *Relating the Cabibbo angle to $\tan\beta$ in a two Higgs-doublet model*, Phys. Rev. D 100 (2019) 075004. <https://doi.org/10.1103/PhysRevD.100.075004>.
- [21] A. E. Cárcamo Hernández, C. O. Dib, U. J. Saldaña-Salazar, *When $\tan\beta$ meets all the mixing angles*, Phys. Lett. B 809 (2020) 135750. <https://doi.org/10.1016/j.physletb.2020.135750>.
- [22] A. E. Cárcamo Hernández *et. al.*, *Fermion masses and mixings and $g - 2$ muon anomaly in a 3-3-1 model with D_4 family symmetry*, Eur. Phys. J. C 82, 769 (2022). <https://doi.org/10.1140/epjc/s10052-022-10639-9>.
- [23] A. Srivastava, M. Levy, and D. Das, *Diluting quark flavor hierarchies using dihedral symmetry*, Eur. Phys. J. C 82, 205 (2022). <https://doi.org/10.1140/epjc/s10052-022-10125-2>.
- [24] G. C. Branco *et al.*, *Theory and phenomenology of two-Higgs-doublet models*, Phys. Rep. 516 (2012) 1–102. <https://doi.org/10.1016/j.physrep.2012.02.002>.
- [25] Lei Wang, Jin Min Yang, and Yang Zhang, *Two-Higgs-doublet models in light of current experiments: a brief review*, Commun. Theor. Phys. 74 (2022), 097202. <https://doi.org/10.1088/1572-9494/ac7fe9>.
- [26] S. Heinemeyer, C. Li, F. Lika, G. Moortgat-Pick, and S. Paasch, *Phenomenology of a 96 GeV Higgs boson in the 2HDM with an additional singlet*, Phys. Rev. D 106 (2022) 075003. <https://doi.org/10.1103/PhysRevD.106.075003>.
- [27] Duarte Azevedo, Thomas Biekötter, P.M. Ferreira, *2HDM interpretations of the CMS diphoton excess at 95 GeV*, arXiv:2305.19716 [hep-ph].
- [28] A. Mondragón, M. Mondragón, and E. Peinado, *Lepton masses, mixings and FCNC in a minimal S_3 -invariant extension of the Standard Model*, Phys.Rev.D 76 (2007) 076003. <https://doi.org/10.1103/PhysRevD.76.076003>.
- [29] J. Kubo, *Super Flavorsymmetry with Multiple Higgs Doublets*, Fortsch.Phys. 61 (2013) 597. <https://doi.org/10.1002/prop.201200119>.
- [30] I. Dorsner *et al.* *New physics models facing lepton flavor violating Higgs decays at the percent level*. J. High Energ. Phys. 2015 (2015) 108. [https://doi.org/10.1007/JHEP06\(2015\)108](https://doi.org/10.1007/JHEP06(2015)108).
- [31] S. Davidson and G. Grenier, *Lepton flavor violating Higgs bosons and $\tau \rightarrow \mu\gamma$* , Phys. Rev. D 81 (2010) 095016. <https://doi.org/10.1103/PhysRevD.81.095016>.
- [32] S. Davidson, *$\mu \rightarrow e\gamma$ in the 2HDM: an exercise in EFT*, Eur. Phys. J. C 76 (2016) 258. <https://doi.org/10.1140/epjc/s10052-016-4076-y>.
- [33] V. V. Vien and H. N. Long, *Multiscalar B-L extension based on S_4 flavor symmetry for neutrino mass and mixing*, Chinese Phys. C 45 (2021) 043112. <https://doi.org/10.1088/1674-1137/abe1c7>.
- [34] H. Ishimori *et. al.*, *Non-Abelian Discrete Symmetries in Particle Physics*, Prog. Theor. Phys. Suppl. 183 (2010) 1. <https://doi.org/10.1143/PTPS.183.1>.

- [35] C. Jarlskog, *Commutator of the Quark Mass Matrices in the Standard Electroweak Model and a Measure of Maximal CP Nonconservation*, *Phys. Rev. Lett.* **55** 1039 (1985). <https://doi.org/10.1103/PhysRevLett.55.1039>.
- [36] M. Mitra, G. Senjanovic and F. Vissani, *Neutrinoless double beta decay and heavy sterile neutrinos*, *Nucl. Phys. B* **856** (2012) 26. <https://doi.org/10.1016/j.nuclphysb.2011.10.035>.
- [37] P. F. de Salas *et al.*, *2020 Global reassessment of the neutrino oscillation picture*, *J. High Energ. Phys.* 2021, 71 (2021). [https://doi.org/10.1007/JHEP02\(2021\)071](https://doi.org/10.1007/JHEP02(2021)071).
- [38] S. R. Choudhury, Shouvik and Hannestad, Steen, *Updated results on neutrino mass and mass hierarchy from cosmology with Planck 2018 likelihoods*, *JCAP* 2007 (2020) 037. <https://doi.org/10.1088/1475-7516/2020/07/037>.
- [39] I. Tanseri *et al.*, *Updated neutrino mass constraints from galaxy clustering and CMB lensing-galaxy cross-correlation measurements*, *JHEAp* 36 (2022) 1. <https://doi.org/10.1016/j.jheap.2022.07.002>.
- [40] S. R. Choudhury and S. Choubey, *JCAP* 1809 (2018) no.09, 017, arXiv: 1806.10832 [astro-ph.CO].
- [41] S. Vagnozzi *et al.*, *Unveiling ν secrets with cosmological data: neutrino masses and mass hierarchy*, *Phys. Rev. D* 96 (2017) 123503. <https://doi.org/10.1103/PhysRevD.96.123503>.
- [42] Elena Giusarma *et al.*, *On the improvement of cosmological neutrino mass bounds*, *Phys. Rev. D* 94 (2016) 083522. <https://doi.org/10.1103/PhysRevD.94.083522>.
- [43] S. Vagnozzi *et al.*, *Constraints on the sum of the neutrino masses in dynamical dark energy models with $w(z) \geq -1$ are tighter than those obtained in Λ CDM*, *Phys. Rev. D* 98 (2018) 083501. <https://doi.org/10.1103/PhysRevD.98.083501>.
- [44] Elena Giusarma *et al.*, *Scale-dependent galaxy bias, CMB lensing-galaxy cross-correlation, and neutrino masses*, *Phys. Rev. D* 98 (2018) 123526. <https://doi.org/10.1103/PhysRevD.98.123526>.
- [45] A. Gando *et al.* (KamLAND-Zen Collaboration), *Search for Majorana Neutrinos Near the Inverted Mass Hierarchy Region with KamLAND-Zen*, *Phys.Rev.Lett.* 117 (2016) 082503. <https://doi.org/10.1103/PhysRevLett.117.082503>.
- [46] M. Agostini *et al.* (GERDA Collaboration), *Probing Majorana neutrinos with double- β decay*, *Science* 365 (2019) 1445. DOI: 10.1126/science.aav8613.
- [47] D. Adams *et al.* (CUORE collaboration), *Improved Limit on Neutrinoless Double-Beta Decay in ^{130}Te with CUORE*, *Phys.Rev.Lett.* 124 (2020) 122501. <https://doi.org/10.1103/PhysRevLett.124.122501>.
- [48] Jun Cao *et al.*, *Towards the meV limit of the effective neutrino mass in neutrinoless double-beta decays*, *Chinese Phys. C* 44 (2020) 031001. <https://doi.org/10.1088/1674-1137/44/3/031001>.
- [49] M. Aker *et al.* (The KATRIN Collaboration), *Direct neutrino-mass measurement with sub-electronvolt sensitivity*, *Nat. Phys.* 18 (2022) 160. <https://doi.org/10.1038/s41567-021-01463-1>.